

Supporting Information

Self-Assembly of Nano- to Macroscopic Metal–Phenolic Materials

Gyeongwon Yun,^{†,‡} Quinn A. Besford,^{†,‡} Stuart T. Johnston,^{§,⊥} Joseph J. Richardson,[†]
Shuaijun Pan,[†] Matthew Biviano,^{||} and Frank Caruso^{*,†}

[†]ARC Centre of Excellence in Convergent Bio-Nano Science and Technology, and the Department of Chemical Engineering, The University of Melbourne, Parkville, Victoria 3010, Australia

[§]Systems Biology Laboratory, School of Mathematics and Statistics, and the Department of Biomedical Engineering, The University of Melbourne, Parkville, Victoria 3010, Australia

[⊥]ARC Centre of Excellence in Convergent Bio-Nano Science and Technology, Melbourne School of Engineering, The University of Melbourne, Parkville, Victoria 3010, Australia

^{||}Department of Chemical Engineering, The University of Melbourne, Parkville, Victoria 3010, Australia

*E-mail: fcaruso@unimelb.edu.au

[‡]These authors contributed equally.

Table of Contents

<u>Section S1: Materials</u>	S3
<u>Section S2: General procedures</u>	S3
<u>Section S3: Film formation using different metal ions and polyphenols</u>	S5
<u>Section S4: Variables influencing growth of the Fe^{III}-TA film</u>	S5
<u>Section S5: Formation of hollow capsules on sacrificial templates</u>	S9
<u>Section S6: Formation of replica particle using CaCO₃ template particles</u>	S10
<u>Section S7: Mechanical tests</u>	S11
<u>Section S8: Permeability test</u>	S12
<u>Section S9. Wettability tests</u>	S12
<u>Section S10: Supporting Figures S1–S29</u>	S14
<u>Section S11: Supporting references</u>	S45

Section S1: Materials

Tannic acid (TA, ACS reagent), gallic acid (GA, 97.5–102.5%), pyrocatechol (PC, $\geq 99.0\%$), pyrogallol (PG, 99.0%), iron(III) chloride hexahydrate ($\text{FeCl}_3 \cdot 6\text{H}_2\text{O}$), europium(III) chloride hexahydrate ($\text{EuCl}_3 \cdot 6\text{H}_2\text{O}$), gallium(III) nitrate hydrate ($\text{Ga}(\text{NO}_3)_3 \cdot x\text{H}_2\text{O}$), indium(III) nitrate hydrate ($\text{In}(\text{NO}_3)_3 \cdot x\text{H}_2\text{O}$), 3-(N-morpholino)propanesulfonic acid (MOPS), ethylenediaminetetraacetic acid (EDTA), polyethyleneimine (PEI, $M_w \sim 10,000$), polystyrene (PS, $M_w \sim 350,000$), poly(sodium 4-styrene sulfonate) (PSS, $M_w \sim 70$ kDa), and fluorescein isothiocyanate (FITC)-dextran with various average molecular weights (20, 70, 250, 2,000 kDa) were purchased from Sigma-Aldrich. Tetrahydrofuran (THF), methanol (MeOH), and acetonitrile (AcCN) were purchased from Chem Supply. Polystyrene (PS) particles (diameter (D) = 3.22 μm , 10% w/w) were purchased from microParticles GmbH. Planar glass substrates (76 mm \times 26 mm) were obtained from Waldemar Knittel. Planar quartz substrates (76 mm \times 25 mm) were purchased from ProSciTech. Gold surfaces were prepared using an Emitech K575x sputter coater. High-purity water with a resistivity of 18.2 $\text{M}\Omega$ cm was obtained from an inline Millipore RiOs/Origin water purification system. All solutions were freshly prepared for immediate use in each experiment.

Section S2: General procedures

Differential interference contrast (DIC) and fluorescence microscopy images were taken with an inverted Olympus IX71 microscope. Confocal laser scanning microscopy (CLSM) images were acquired with a Leica TCS SP2 laser scanning microscope. Atomic force microscopy (AFM) experiments were carried out with a JPK NanoWizard II BioAFM. Typical scans were conducted in intermittent contact mode with MikroMasch silicon cantilevers (NSC/CSC). The film thickness and roughness of the metal–phenolic films were analyzed using JPK SPM image processing software (version V.3.3.32). AFM force measurements were carried out

with an MFP-3D from Asylum Research using biosphere cantilevers that have a 50 nm radius spherical tip and a nominal spring constant of 40 N m⁻¹ (NanoTools, Munich). Transmission electron microscopy (TEM) images and energy-dispersive X-ray spectroscopy (EDX) profiles were acquired using a FEI Tecnai F20 instrument with an operation voltage of 200 kV. Scanning electron microscopy (SEM) images were obtained using a FEI Quanta 200 ESEM with an operation voltage of 10 kV. Scanning helium ion microscopy images were obtained using a Zeiss Orion Nanofab helium ion microscope. UV-Visible absorption measurements were carried out on an Analytik Jena SPECORD 250 PL. Mass spectra were obtained using a Bruker Autoflex III smartbeam MALDI TOF mass spectrometer operating in positive linear mode. Optical waveguide lightmode spectroscopy (OWLS) measurements were performed with an OWLS 210 instrument (MicroVacuum, Budapest, Hungary), programmed with Biosense 2.6 software. Contact angle measurements were made using a DataPhysics OCA 20 tensiometer. The static contact angles were recorded with OCA software using the sessile drop profile. X-ray photoelectron spectroscopy was performed on a VG ESCALAB220i-XL spectrometer equipped with a hemispherical analyzer. The incident radiation was monochromatic Al K α X-rays (1486.6 eV) at 220 W (22 mA and 10 kV). Survey (wide) and high-resolution (narrow) scans were taken at analyzer pass energies of 100 and 50 eV, respectively. Survey scans were carried out with a 1.0 eV step size and a 100 ms dwell time. Narrow high-resolution scans were run over a 20 eV binding energy range with a 0.05 eV step size and a 250 ms dwell time. Base pressure in the analysis chamber was below 8.0×10^{-9} mbar. A low-energy flood gun was used to minimize surface charging. All data were processed using CasaXPS software, and the energy calibration was referenced to the C 1s peak at 285.0 eV. For the sample preparation, films were prepared on planar glass substrates and allowed to air dry.

Section S3: Film formation using different metal ions and polyphenols

1. Different metal ions: All solutions were freshly prepared for immediate use. Aliquots (5 mL) of fresh metal in water (37 mM of EuCl_3 , $\text{Ga}(\text{NO}_3)_3$, or $\text{In}(\text{NO}_3)_3$ solution), TA in water (23.5 mM), and MOPS buffer (10 mM, pH 8) were added to water (5 mL), and the solution was vigorously mixed by a vortex mixer for 10 s. In the purification step, the metal–TA solutions were centrifuged at 2,000 g for 5 min and then filtered with a syringe filter with a 0.22 μm pore size to remove precipitates from the solutions. Planar glass substrates were immersed in each purified metal–TA solution in a 50 mL tube for 20 h. The coated substrates were washed with water thrice to remove excess metal ions and TA. The coated substrates were subsequently immersed in MOPS buffer (40 mL, 10 mM, pH 8) in a 50 mL tube to strongly cross-link the metal ions with phenolic molecules.

2. Different polyphenols: Aliquots (5 mL) of fresh $\text{FeCl}_3 \cdot 6\text{H}_2\text{O}$ in water (37 mM) and polyphenol in water (37 mM of GA, PC, or PG solution) were added to water (10 mL), and the solution was vigorously mixed by a vortex mixer for 10 s. In the purification step, the Fe^{III} –polyphenol solutions were centrifuged at 2,000 g for 5 min and then filtered with a syringe filter with a 0.22 μm pore size to remove precipitates from the solutions. Planar glass substrates were immersed in each purified Fe^{III} –polyphenol solution in a 50 mL tube for 72 h. The coated substrates were washed with water thrice to remove excess Fe^{III} and polyphenols. The coated substrates were subsequently immersed in MOPS buffer (40 mL, 10 mM, pH 8) in a 50 mL tube to strongly cross-link the metal ions with phenolic molecules.

Section S4: Variables influencing growth of the Fe^{III} –TA film

1. Concentration effect. All solutions were freshly prepared for immediate use. An aliquot (5 mL) of $\text{FeCl}_3 \cdot 6\text{H}_2\text{O}$ in water (37, 56.5, or 75.5 mM) was added to water (10 mL). Following

this, an aliquot (5 mL) of TA in water (23.5, 35.3, or 47.2 mM) was added, and the Fe^{III}-TA solution was vigorously mixed by a vortex mixer for 10 s. The ratio of Fe^{III} to TA was 1:1.6. The Fe^{III}-TA solution was centrifuged at 2,000 g for 5 min and then filtered with a syringe filter with a 0.22 μm pore size to remove precipitates from the solution. Planar glass substrates were immersed in the purified Fe^{III}-TA solution in a 50 mL tube. The coated substrates were washed with water thrice to remove excess Fe^{III} and TA. The coated substrates were subsequently immersed in MOPS buffer (40 mL, 10 mM, pH 8) in a 50 mL tube to strongly cross-link the metal ions with phenolic molecules.

2. pH effect. All solutions were freshly prepared for immediate use. Aliquots (5 mL) of FeCl₃·6H₂O (37 mM) and TA (23.5 mM) in water were added to water (10 mL), and the solution was vigorously mixed by a vortex mixer for 10 s. The pH of the Fe^{III}-TA solution was controlled by adding 1 M HCl or 1 M NaOH solution. The Fe^{III}-TA solution was centrifuged at 2,000 g for 5 min and then filtered with a syringe filter with a 0.22 μm pore size to remove precipitates from the solution. Planar glass substrates were immersed in the purified Fe^{III}-TA solution in a 50 mL tube for 20 h. The coated substrates were washed with water thrice to remove excess Fe^{III} and TA. The coated substrates were subsequently immersed in MOPS buffer (40 mL, 10 mM, pH 8) in a 50 mL tube to strongly cross-link the metal ions with phenolic molecules.

3. Substrate effect. All solutions were freshly prepared for immediate use. Aliquots (5 mL) of FeCl₃·6H₂O (37 mM) and TA (23.5 mM) in water were added to water (10 mL), and the solution was vigorously mixed by a vortex mixer for 10 s. The Fe^{III}-TA solution was centrifuged at 2,000 g for 5 min and then filtered with a syringe filter with a 0.22 μm pore size to remove precipitates from the solution. Planar glass, PEI, gold, PS, or quartz substrates were immersed in the purified Fe^{III}-TA solution in a 50 mL tube for 20 h. The coated

substrates were washed with water thrice to remove excess Fe^{III} and TA. The coated substrates were subsequently immersed in MOPS buffer (40 mL, 10 mM, pH 8) in a 50 mL tube to strongly cross-link the metal ions with phenolic molecules.

- a) PEI substrates: Ethanol-cleaned glass substrates were immersed in PEI solution (1 mg mL^{-1} , 0.5 M NaCl in water) for 15 min, rinsed in water, and dried in air flow.
- b) Gold substrates: Ethanol-cleaned glass substrates were coated with gold using a sputter coater at 45 mA for 40 s.
- c) PS substrates: Ethanol-cleaned glass substrates were coated with a PS layer by dipping the substrates in PS solution (50 mg mL^{-1} in THF) and immediately dried in air flow.

4. Solvent effect. All solutions were freshly prepared for immediate use. Aliquots (1.25 mL) of $\text{FeCl}_3 \cdot 6\text{H}_2\text{O}$ (37 mM) and TA (23.5 mM) in AcCN, MeOH, or water were added to AcCN (2.5 mL), MeOH (2.5 mL), or water (2.5 mL), respectively. Each solution was vigorously mixed by a vortex mixer for 10 s, centrifuged at 2,000 g for 5 min, and filtered with a 0.22 μm pore size syringe filter to remove precipitates from the solution. Aqueous PS template ($D = 3.22 \mu\text{m}$) suspension (0.5 mL) was added to each purified Fe^{III} -TA solution (5 mL) and stirred for 30 min. The particles were washed with AcCN (5 mL), MeOH (5 mL), or water (5 mL) thrice to remove excess Fe^{III} and TA. The pH of the suspensions was subsequently raised using MOPS buffer (5 mL, 10 mM, pH 8) to strongly cross-link the metal ions with phenolic molecules. In the washing step, the particles were centrifuged (2,000 g, 30 s), the supernatant was completely removed, and the pellets were vortexed for 10 s. To obtain capsules, the PS was removed by washing with THF four times. In each THF washing step, the pellets were first vortexed for 10 s, then THF (5 mL) was then added to the pellet, and the pellet was resuspended through gentle pipetting (at least 20 times). This suspension was then kept on the

rotator for 30 min. Finally, the particles were centrifuged (2,000 g, 30 s), the supernatant was removed, and the process was repeated four times.

5. TA:Fe^{III} molar ratio effect. All solutions were freshly prepared for immediate use. Aliquots (1 mL) of FeCl₃·6H₂O (4.7–470 mM) and TA (23.5 mM) in water were added to water (2 mL), and the solutions were vigorously mixed by a vortex mixer for 10 s. The Fe^{III}–TA solutions were centrifuged at 2,000 g for 5 min and then filtered with a syringe filter with a 0.22 μm pore size to remove precipitates from the solutions. Aqueous PS template ($D = 3.22$ μm) suspension (0.4 mL) was added to the purified Fe^{III}–TA solution (4 mL) and stirred for 30 min. The particles were washed with water (5 mL) thrice to remove excess Fe^{III} and TA. The pH of the suspensions was subsequently raised using MOPS buffer (4 mL, 10 mM, pH 8) to strongly cross-link the metal ions with phenolic molecules. In the washing step, the particles were centrifuged (2,000 g, 30 s), the supernatant was completely removed, and the pellets were vortexed for 10 s. To obtain capsules, the PS was removed by washing with THF four times. In each THF washing step, the pellets were first vortexed for 10 s, THF (4 mL) was then added to the pellet, and the pellet was resuspended through gentle pipetting (at least 20 times). This suspension was then kept on the rotator for 30 min. Finally, the particles were centrifuged (2,000 g, 30 s), the supernatant was removed, and the process was repeated four times.

6. Temperature effect. All solutions were freshly prepared for immediate use. Aliquots (1.25 mL) of FeCl₃·6H₂O (37 mM) and TA (23.5 mM) in water were added to water (2.5 mL), and the solution was vigorously mixed by a vortex mixer for 10 s. The Fe^{III}–TA solutions were centrifuged at 2,000 g for 5 min and then filtered with a syringe filter with a 0.22 μm pore size to remove precipitates from the solution. Then, the temperature of solutions was controlled by a water bath and stabilized for 30 min. Aqueous PS template ($D = 3.22$ μm)

suspension (0.5 mL) was added to each purified Fe^{III}-TA solution (5 mL) and stirred for 30 min. The particles were washed with water (5 mL) thrice to remove excess Fe^{III} and TA. The pH of the suspensions was subsequently raised using MOPS buffer (5 mL, 10 mM, pH 8) to strongly cross-link the metal ions with phenolic molecules. In the washing step, the particles were centrifuged (2,000 g, 30 s), the supernatant was completely removed, and the pellets were vortexed for 10 s. To obtain capsules, the PS was removed by washing with THF four times. In each THF washing step, the pellets were first vortexed for 10 s, THF (5 mL) was then added to the pellet, and the pellet was resuspended through gentle pipetting (at least 20 times). This suspension was then kept on the rotator for 30 min. Finally, the particles were centrifuged (2,000 g, 30 s), the supernatant was removed, and the process was repeated four times.

Section S5: Formation of hollow capsules on sacrificial templates

All solutions were freshly prepared for immediate use. Aliquots (1.25 mL) of FeCl₃·6H₂O (37 mM) and TA (23.5 mM) in water were added to water (2.5 mL), and the solution was vigorously mixed by a vortex mixer for 10 s. The Fe^{III}-TA solution was centrifuged at 2,000 g for 5 min and then filtered with a syringe filter with a 0.22 μm pore size to remove precipitates from the solution. Aqueous PS template ($D = 3.22 \mu\text{m}$) suspension (0.5 mL) was added to the purified Fe^{III}-TA solution (5 mL) under stirring. The particles were washed with water (5 mL) thrice to remove excess Fe^{III} and TA. The pH of the suspensions was subsequently raised using MOPS buffer (5 mL, 10 mM, pH 8) to strongly cross-link the metal ions with phenolic molecules. In the washing step, the particles were centrifuged (2,000 g, 30 s), the supernatant was completely removed, and the pellets were vortexed for 10 s. To obtain capsules, the PS template was removed by washing with THF four times. In each THF washing step, the pellets were vortexed for 10 s, THF (5 mL) was added to the pellet, and the

pellet was resuspended through gentle pipetting (at least 20 times). This suspension was then kept on the rotator for 30 min. Finally, the particles were centrifuged (2,000 g, 30 s), the supernatant was removed, and the process was repeated four times.

Section S6: Formation of replica particle using CaCO₃ template particles

1. Preparation of CaCO₃ template particles. For the preparation of PSS-stabilized CaCO₃ particles, sodium carbonate (2.4 mL, 1 M) and PSS (200 mL, 1 mg mL⁻¹) were mixed in a 200 mL beaker under vigorous stirring. Then, CaCl₂ in water (4.8 mL, 1 M) was rapidly added. After stirring for 60 s, the PSS-stabilized CaCO₃ particles were washed thrice with water to remove unreacted material and resuspended in water. The obtained PSS-stabilized CaCO₃ particles were then calcined in air at 550 °C for 6 h to burn off PSS and other organic materials, yielding nanoporous CaCO₃ particles.

2. Synthesis of Fe^{III}-TA replica particles. All solutions were freshly prepared for immediate use. Aliquots (1.25 mL) of FeCl₃·6H₂O (37 mM) and TA (23.5 mM) in water were added to water (2.5 mL), and the solution was vigorously mixed by a vortex mixer for 10 s. The Fe^{III}-TA solution was centrifuged at 2,000 g for 5 min and then filtered with a syringe filter with a 0.22 μm pore size to remove precipitates from the solution. Then, CaCO₃ template particles in water (0.5 mL, 5 mg mL⁻¹) were added to the purified Fe^{III}-TA solution (5 mL) under stirring for 1 h. The particles were then washed with water (5 mL) thrice to remove excess Fe^{III} and TA. The pH of the suspensions was subsequently raised using MOPS buffer (5 mL, 10 mM, pH 8) to strongly cross-link the metal ions with phenolic molecules. In the washing step, the particles were centrifuged (2,000 g, 30 s), the supernatant was completely removed, and the pellets were vortexed for 10 s. To obtain the Fe^{III}-TA replica particles, the CaCO₃ templates were removed by washing with EDTA twice. In each EDTA washing step, the pellets were

first vortexed for 10 s, and then EDTA (5 mL, 100 mM, pH 8) was added to the pellet, and the pellet was resuspended through gentle pipetting (at least 20 times). Finally, the Fe^{III}-TA replica particles were spun down by centrifugation (2,000 g, 60 s), and the remaining pellet was washed and redispersed in the desired buffer solutions. The CaCO₃ templates were removed, which was confirmed by the extremely low concentrations of Ca in the particle (~0.3%, atomic ratio) based on EDX analysis.

Section S7: Mechanical tests

To investigate the compressional behavior and topographical variability of the Fe^{III}-TA materials, AFM force measurements were performed in air with an MFP-3D from Asylum Research using biosphere cantilevers that have a 50 nm radius spherical tip and a nominal spring constant of 40 N m⁻¹ (NanoTools, Munich). Prior to use, the cantilevers were washed consecutively in ethanol and water. The spring constant can then be determined via the thermal noise method¹ after the optical lever sensitivity is calibrated using a clean glass substrate.

A map of the force vs. indentation across many points were taken at a space of 2 μm between indentation sites, across the surface of the Fe^{III}-TA materials, where the probe was raster scanned above the sample with a constant indentation velocity of 2 μm s⁻¹. The resultant curves are a function of force vs. Z piezo sensor displacement, where the indentation depth can be determined by subtracting the deflection from the Z piezo sensor displacement. Owing to low adhesion, the Hertz model was chosen to estimate the Young's modulus of the material from the force vs. indentation data as follows:

$$F = \frac{4}{3} \frac{E}{(1-\nu^2)} R^{\frac{1}{2}} d^{\frac{3}{2}}$$

where E is the elastic modulus (Pa), ν is Poisson's ratio, R is the radius of the indenter (m), and d is the indentation depth (m). As Poisson's ratio is unknown, a value of 0.4 was used.²

To ensure the validity of the Hertz model, the areas used for compressional analysis were imaged prior to compression and were found to have a root mean square roughness of less than 1.5 nm within a $100 \times 100 \text{ nm}^2$ area, where the measured force was averaged over at least 10 nm of indentation into the film. As the material showed significant plastic deformation, the retract curve was used to determine material properties. The thickness of the material was determined prior to all measurements to ensure that the thickness of the material was at least $2 \text{ }\mu\text{m}$ so that no substrate effects were seen.²

Section S8: Permeability test

A dispersion of the Fe^{III} -TA capsules (prepared from PS templates, $D = 3.22 \text{ }\mu\text{m}$) was mixed with an equal volume of FITC-dextran solution (1 mg mL^{-1}). CLSM images of the capsules were taken within 10 min after mixing; capsules with dark interiors were considered to be impermeable, whereas capsules with interiors of similar fluorescence intensity to that of the outer environment were considered to be permeable.

Section S9. Wettability tests

1. Thickness effect. An aliquot (5 mL) of $\text{FeCl}_3 \cdot 6\text{H}_2\text{O}$ in water (37, 56.5, or 75.5 mM) was added to water (10 mL), followed by the addition of TA in water (5 mL; 23.5, 35.3, or 47.2 mM). The Fe^{III} -TA solution was vigorously mixed by a vortex mixer for 10 s. The ratio of Fe^{III} to TA was 1:1.6. The Fe^{III} -TA solution was centrifuged at 2,000 *g* for 5 min and then filtered with a syringe filter with a $0.22 \text{ }\mu\text{m}$ pore size to remove precipitates from the Fe^{III} -TA solution. Planar glass substrates were immersed in the purified Fe^{III} -TA solution in a 50 mL tube for 89 h. The coated substrates were washed with water thrice to remove excess Fe^{III} and TA. The coated substrates were subsequently immersed in MOPS buffer (40 mL, 10 mM, pH 8) in a 50 mL tube to strongly cross-link the metal ions with phenolic molecules.

2. Metal ion and ligand effect. The fabrication conditions were described in Section S4.

3. Control sample. Control sample of the Fe^{III}-TA film on planar glass was prepared by following literature precedures.³ A planar glass substrate (26 mm × 26 mm) was soaked in water (19.6 mL) in a 50 mL tube. Aliquots (0.2 mL) of FeCl₃·6H₂O (37 mM) and TA (23.5 mM) in water were added to this aqueous solution. The solution was vigorously mixed by a vortex mixer for 10 s immediately after the individual additions of FeCl₃·6H₂O and TA. The coated substrates were subsequently immersed in MOPS buffer (40 mL, 10 mM, pH 8) in a 50 mL tube to strongly cross-link the metal ions with phenolic molecules. Then, the substrates were rinsed with water. This coating process was repeated five times.

Section S10: Supporting Figures S1–S29

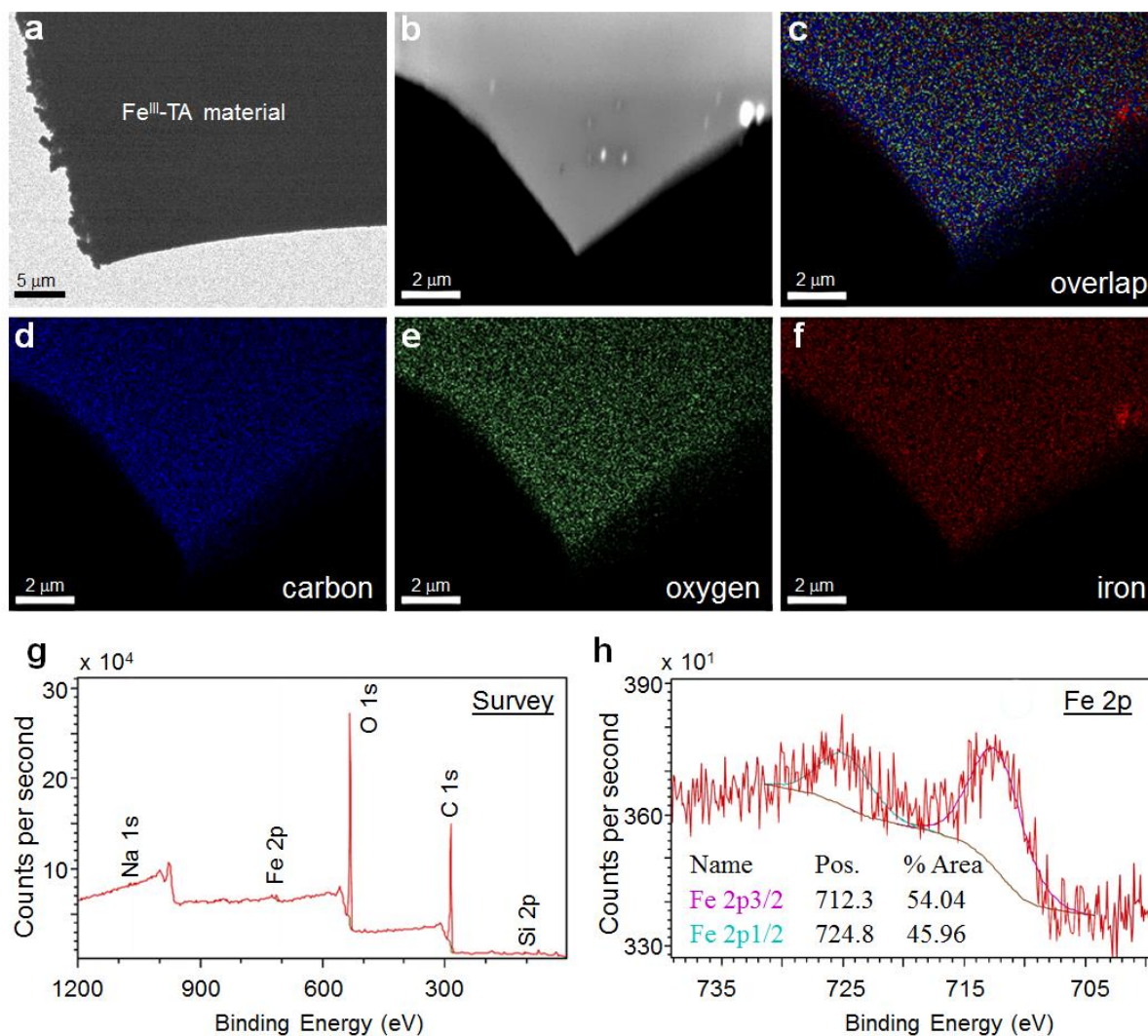


Figure S1. TEM and EDX mapping images, and X-ray photoelectron spectroscopy spectra of a Fe^{III}-TA film. (a–f) Representative TEM (a), high-angle annular dark-field (HAADF) (b), EDX elemental mapping images of a Fe^{III}-TA film on a TEM grid (c–f). (g) Survey spectrum. (h) Fe 2p core level spectrum showing the presence of Fe^{III} in the Fe^{III}-TA film.⁴

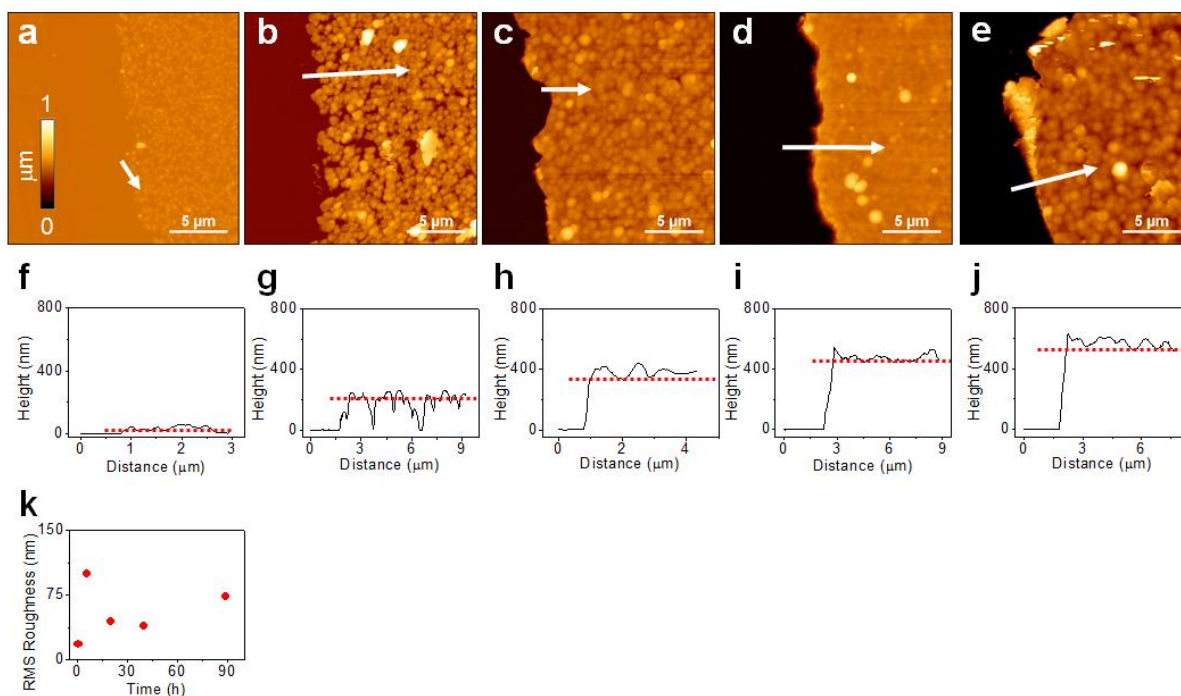


Figure S2. AFM images and corresponding height profiles of a scratched zone of a Fe^{III}-TA film on planar glass substrates at different immersion times: 40 min (a, f), 6 h (b, g), 20 h (c, h), 40 h (d, i) and 89 h (e, j). (k) Surface roughness of Fe^{III}-TA films prepared at different immersion times.

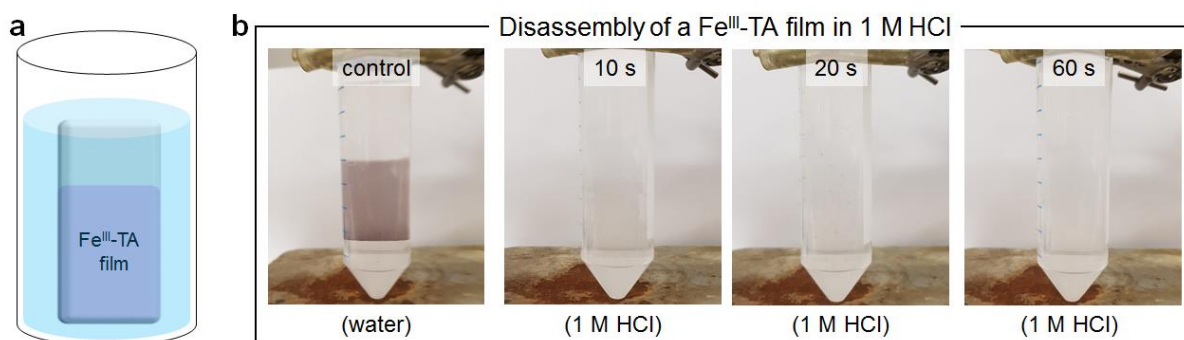


Figure S3. pH-Triggered disassembly of a Fe^{III}-TA film on a planar glass substrate. (a) Schematic of the disassembly test of a Fe^{III}-TA film in 1 M HCl solution. (b) Digital photographs of the disassembly of the Fe^{III}-TA film as a function of time.

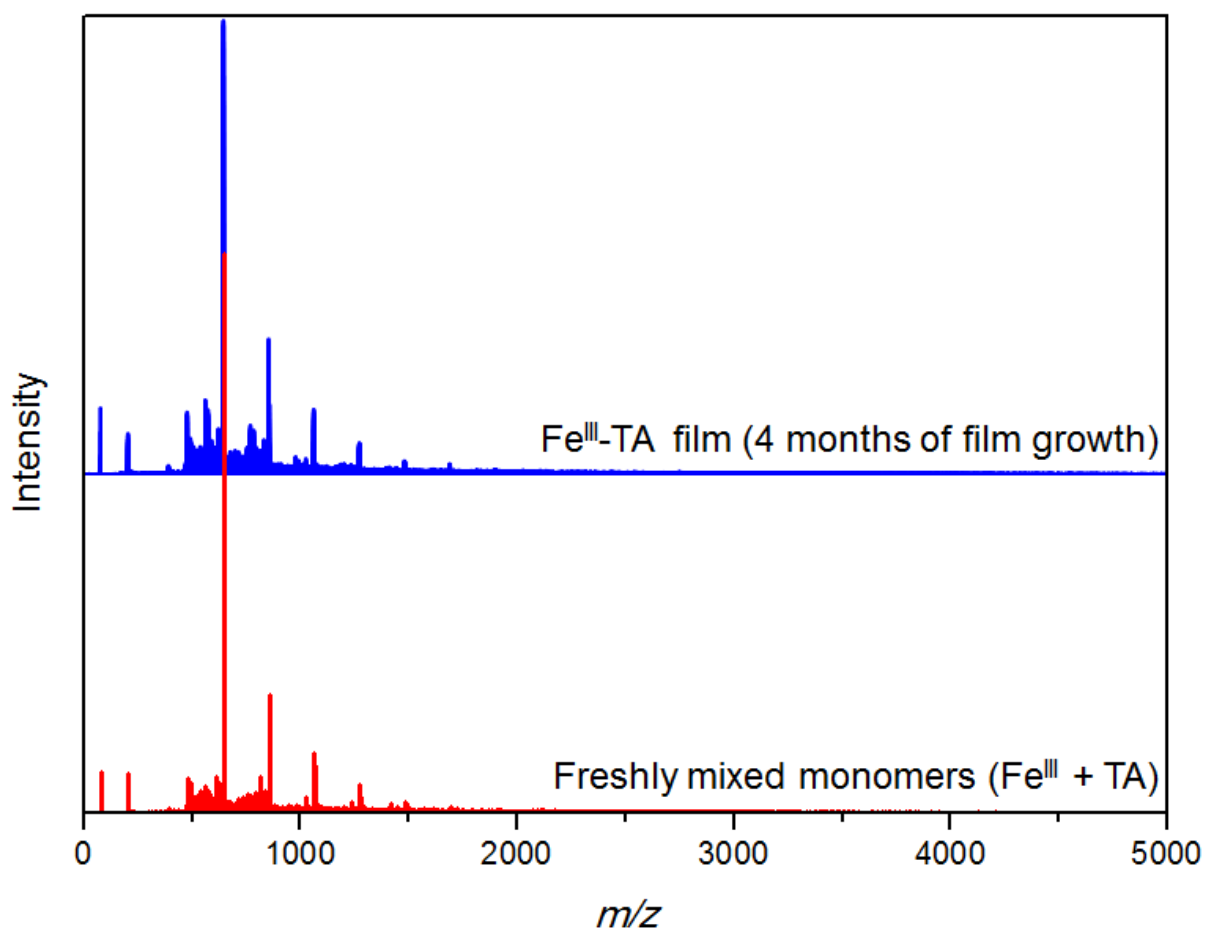


Figure S4. Matrix-assisted laser desorption ionization–time-of-flight mass spectra of a Fe^{III}–TA film (blue) and freshly mixed monomers of Fe^{III} and TA (red) after disassembling the Fe^{III}–TA complexes with EDTA (20 mL, 100 mM, pH 7).

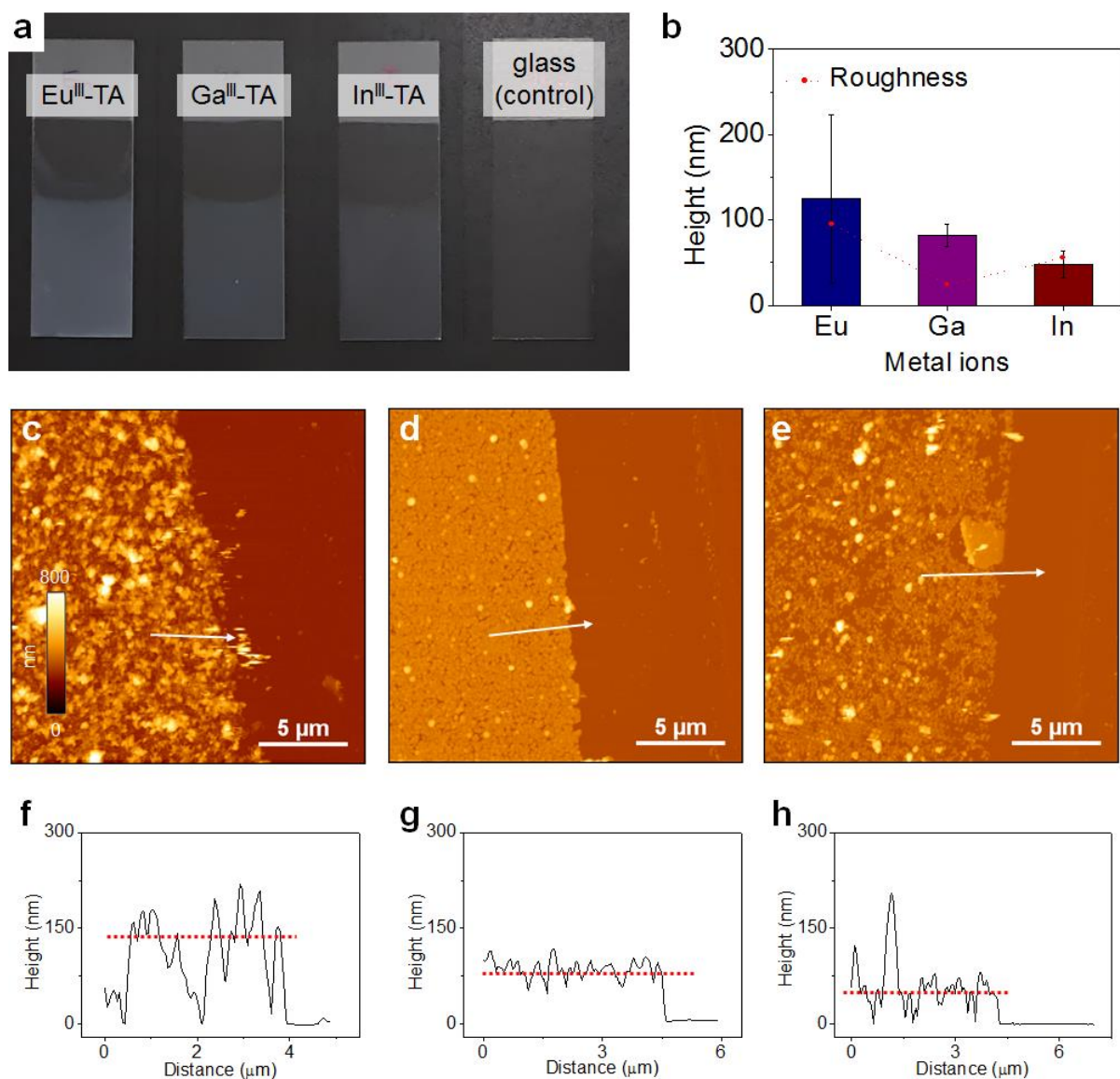


Figure S5. Formation of metal-TA film using different metal ions. (a, b) Digital photograph and thickness of the metal-TA films obtained using different metal ions as measured by AFM height profiles seen in (c-h). (c-h) AFM images and corresponding height profiles of the metal-TA films: Eu^{III}-TA (c, f), Ga^{III}-TA (d, g), and In^{III}-TA (e, h).

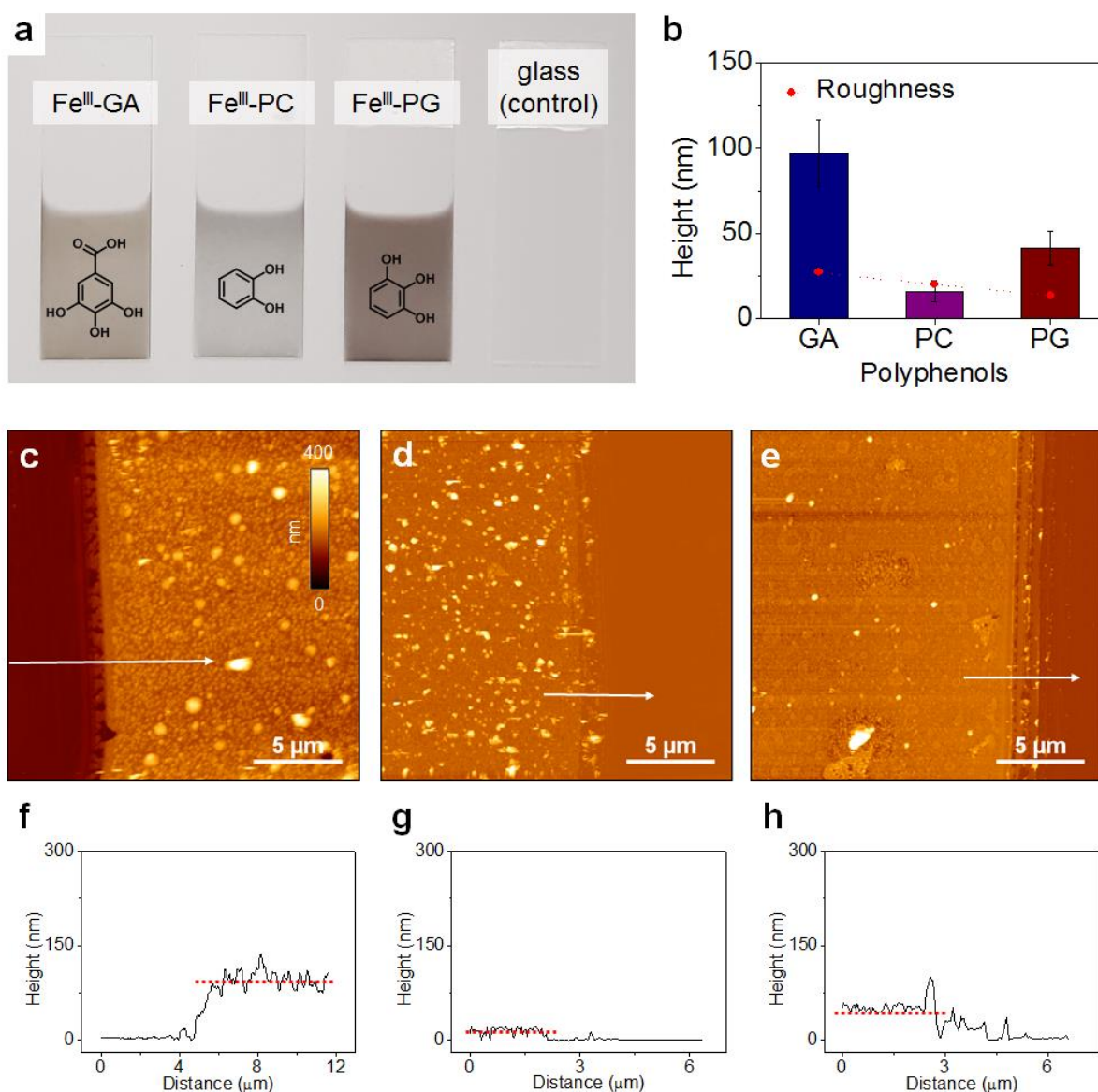


Figure S6. Formation of Fe^{III}-phenolic film using different polyphenols. (a, b) Digital photograph and thickness of the Fe^{III}-TA films obtained using different polyphenols as measured by AFM height profiles seen in (c–h). (c–h) AFM images and corresponding height profiles of the Fe^{III}-phenolic films: Fe^{III}-GA (c, f), Fe^{III}-PC (d, g), and Fe^{III}-PG (e, h).

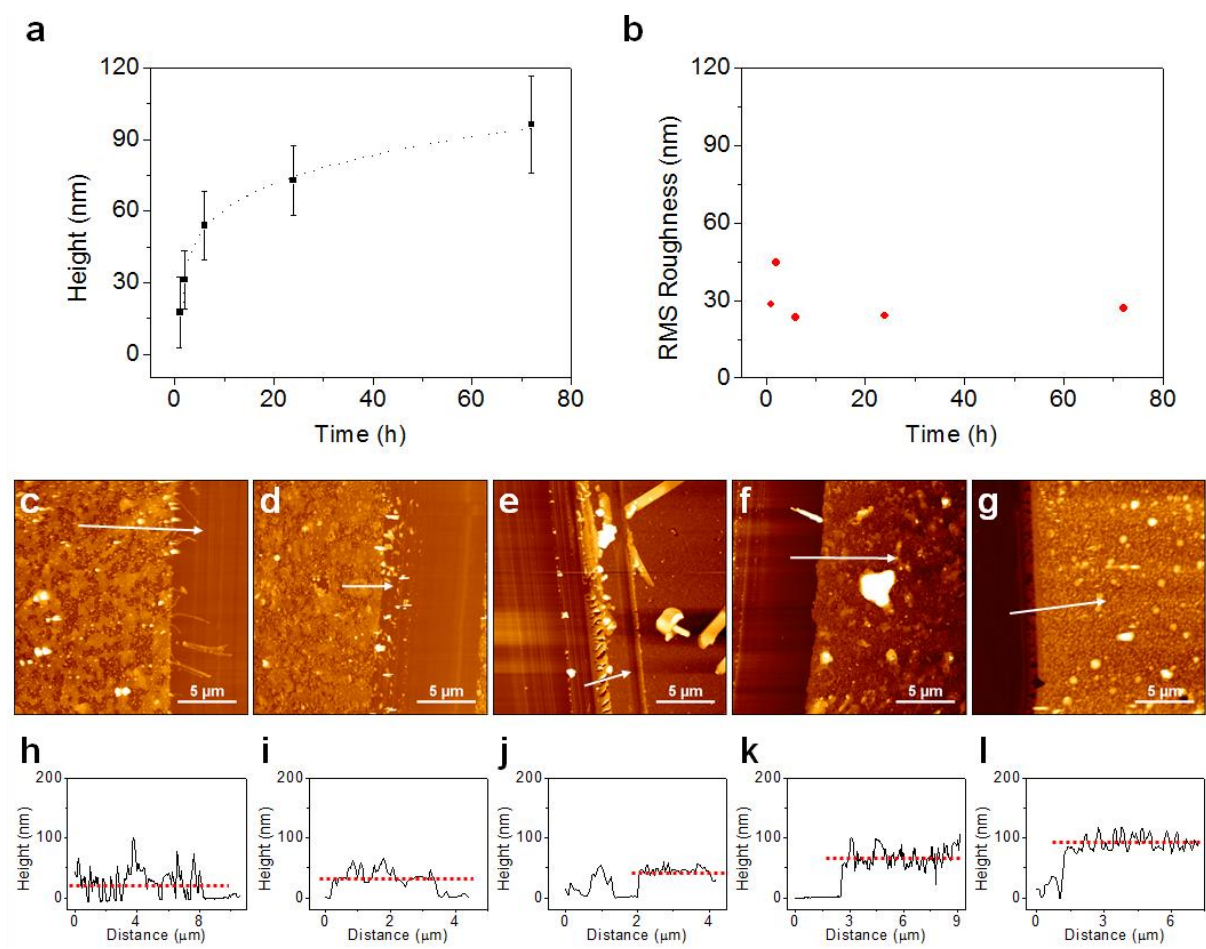


Figure S7. Thickness profile of Fe^{III}-GA films on glass substrates. (a, b) Thickness-time profile and corresponding surface roughness of Fe^{III}-GA films on glass substrates measured by AFM. (c-l) AFM images and corresponding height profiles of a scratched zone of Fe^{III}-GA films on planar glass substrates at different immersion times: 1 h (c, h), 2 h (d, i), 6 h (e, j), 24 h (f, k), and 72 h (g, l).

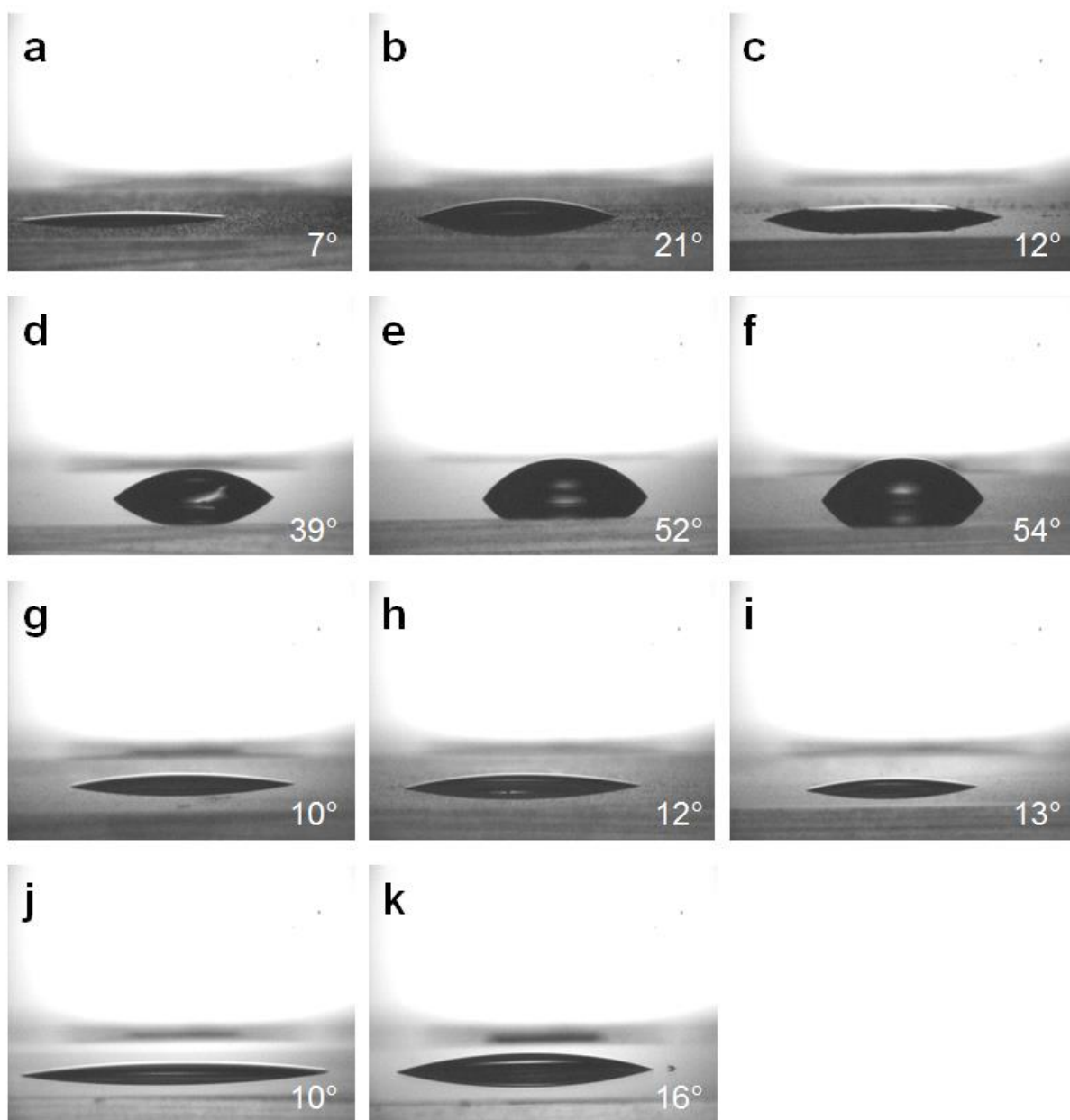


Figure S8. Water droplets on various metal-phenolic films on planar glass substrates. (a–c) Thickness effect of Fe^{III} -TA films on wettability: ~ 100 nm (a), ~ 300 nm (b), and ~ 600 nm (c). (d–f) Ligand effect on wettability: Fe^{III} -GA film (d), Fe^{III} -PC film (e), and Fe^{III} -PG film (f). (g–i) Metal ion effect on wettability: Eu^{III} -TA film (g), Ga^{III} -TA film (h), and In^{III} -TA film (i). (j, k) Control: glass (j) and Fe^{III} -TA film prepared by following literature procedures³ (k).

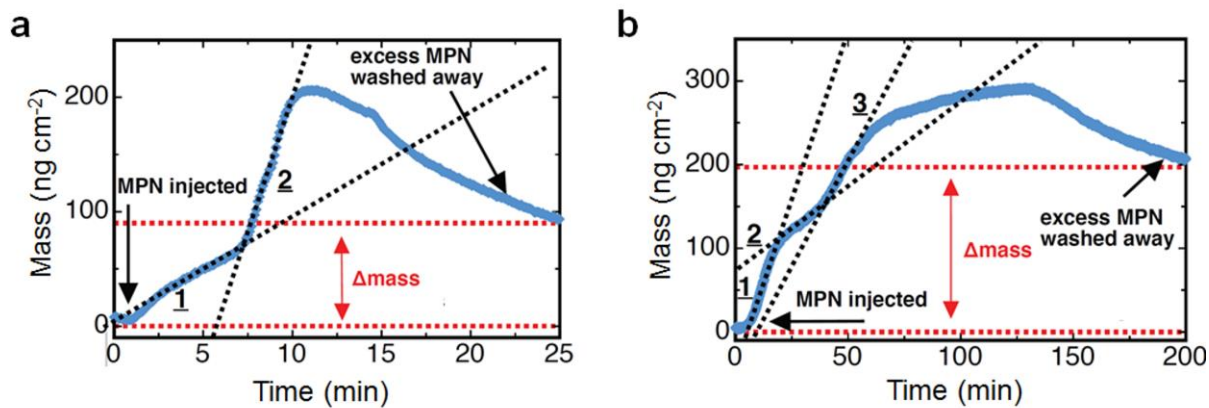


Figure S9. OWLS measurements of the absorbed mass on a silica substrate. Injection flow rate: 500 μL h⁻¹ (a) and 50 μL h⁻¹ (b). At a high flow rate (500 μL h⁻¹), Fe^{III}-TA complexes were deposited on the silica substrate at a mass of about 100 ng cm⁻², whereas at a lower flow rate (50 μL h⁻¹), but with the same injection volume, Fe^{III}-TA complexes were deposited at a mass of ~200 ng cm⁻².

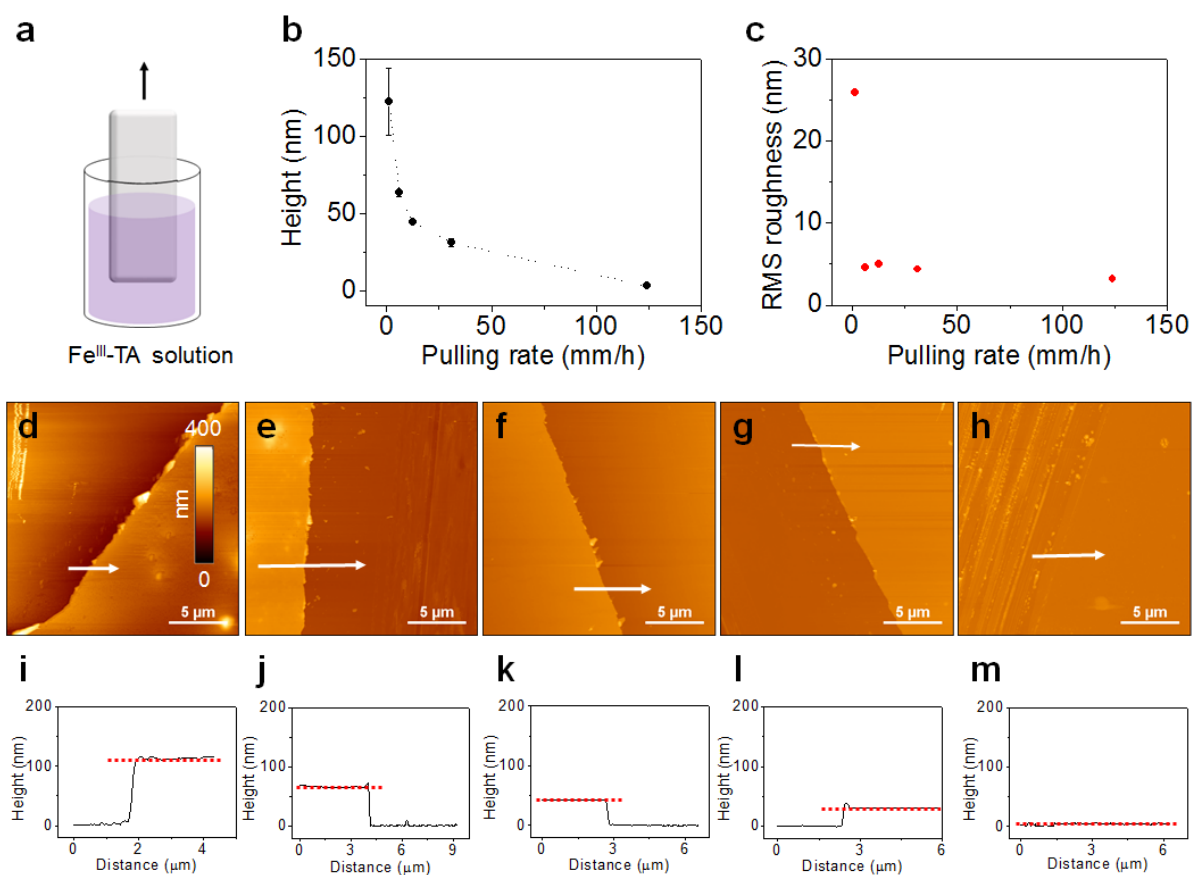


Figure S10. Substrate withdrawal rate effect on Fe^{III} -TA film formation on planar substrates. (a) Schematic of the Fe^{III} -TA film deposition by pull-out method. (b, c) Thickness–pulling rate profile and corresponding surface roughness of Fe^{III} -TA films on glass substrates as measured by AFM. (d–m) AFM height images and corresponding height profiles of a scratched zone of Fe^{III} -TA film. Withdrawal rate: 1.24 mm h^{-1} (d, i), 6.2 mm h^{-1} (e, j), 12.4 mm h^{-1} (f, k), 31 mm h^{-1} (g, l) and 124 mm h^{-1} (h, m). At withdrawal rates of 1.24 , 12.4 , and 124 mm h^{-1} , films with average thicknesses of 122 ± 22 , 44 ± 1 , and $3 \pm 1 \text{ nm}$ were produced, respectively.

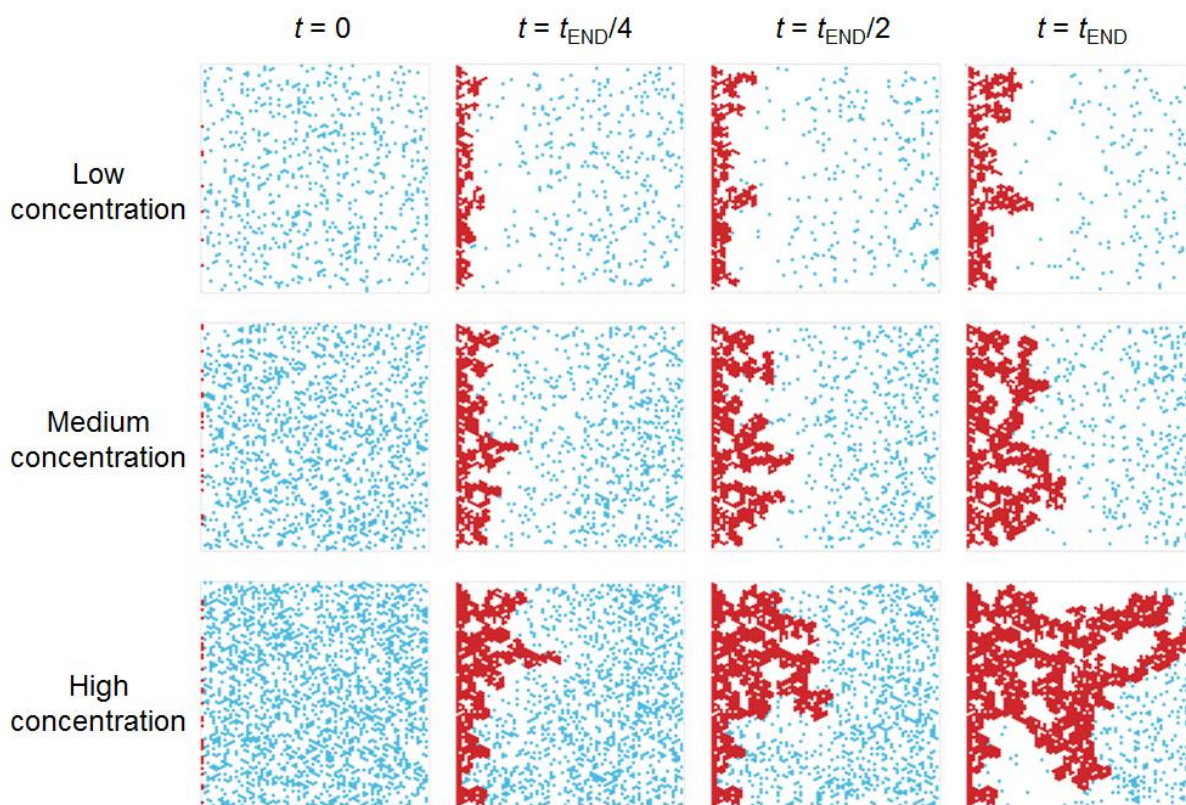


Figure S11. Snapshots of the lattice-based model of concentration effect on film formation.

The average thickness of the film increased with increasing concentrations of reactants.

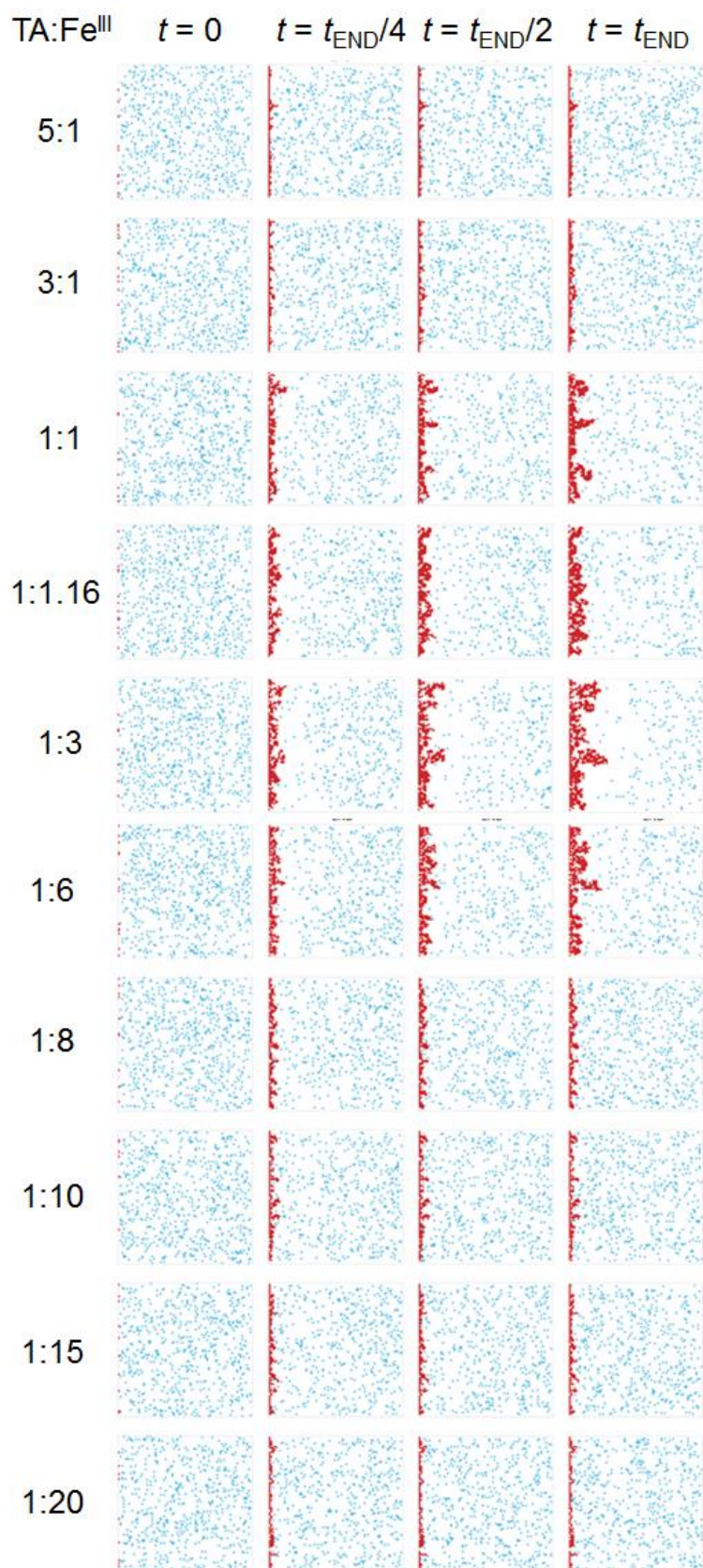


Figure S12. Snapshots of the lattice-based model of TA:Fe^{III} ratio effect on film formation.

The film thickness was greatest at a TA:Fe^{III} molar ratio of 1:3.

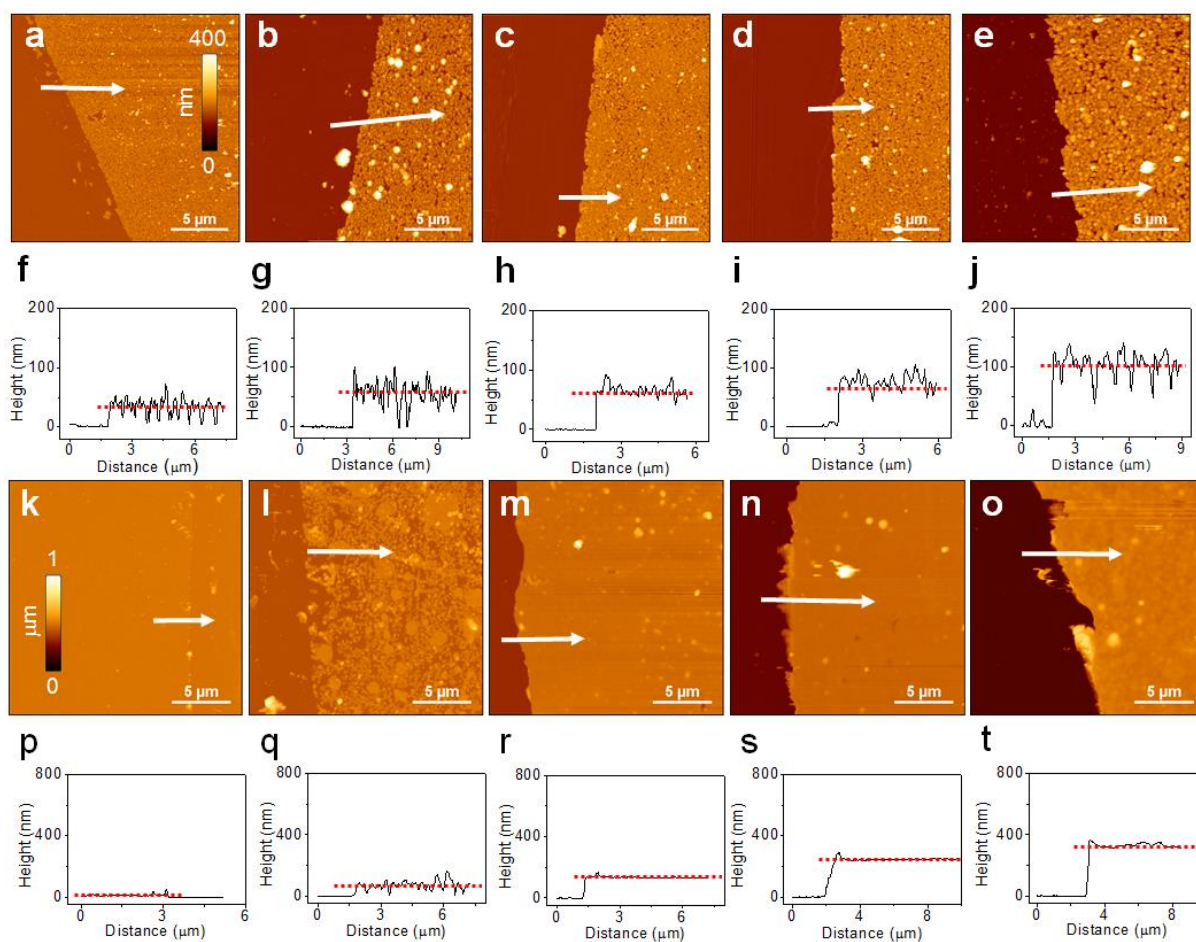


Figure S13. Effect of concentration on Fe^{III}-TA film formation on planar substrates at a given TA:Fe^{III} ratio (1:1.6). (a–j) AFM height images and corresponding height profiles of a scratched zone of an Fe^{III}-TA film formed on a glass substrate (5.9 mM TA; immersion times 40 min, 7 h, 20 h, 40 h, and 89 h, respectively). (k–t) AFM height images and corresponding height profiles of a scratched zone of the Fe^{III}-TA film formed on a glass substrate (8.8 mM TA; immersion times 40 min, 6 h, 20 h, 46 h, and 89 h, respectively).

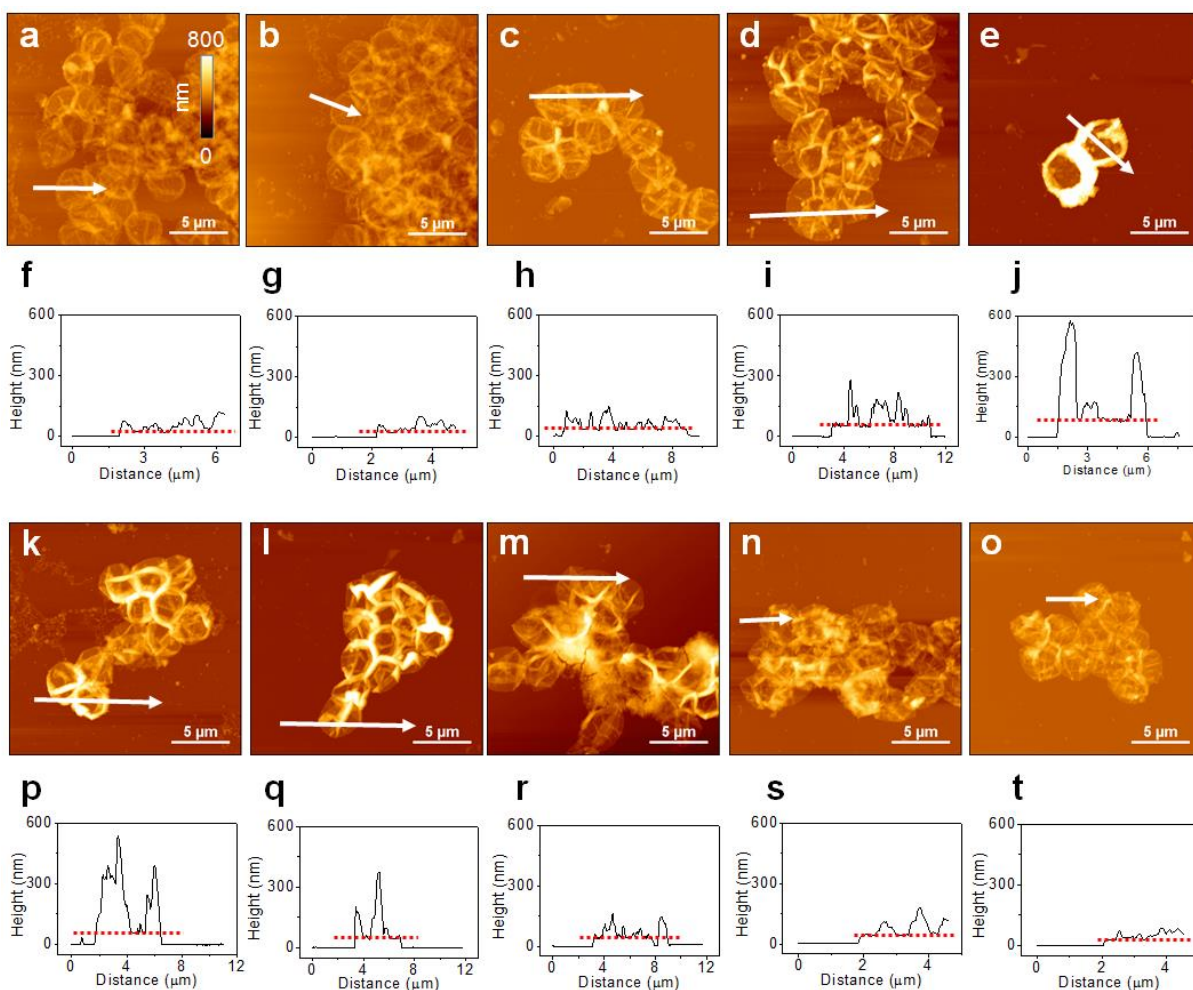


Figure S14. Effect of TA:Fe^{III} molar ratio on Fe^{III}-TA film formation on sacrificial PS particles. (a–t) AFM height images and corresponding height profiles of hollow Fe^{III}-TA capsules formed at different TA:Fe^{III} molar ratios: 5:1 (a, f), 3:1 (b, g), 1:1 (c, h), 1:1.6 (d, i), 1:3 (e, j), 1:6 (k, p), 1:8 (l, q), 1: 10 (m, r), 1:15 (n, s), and 1:20 (o, t).

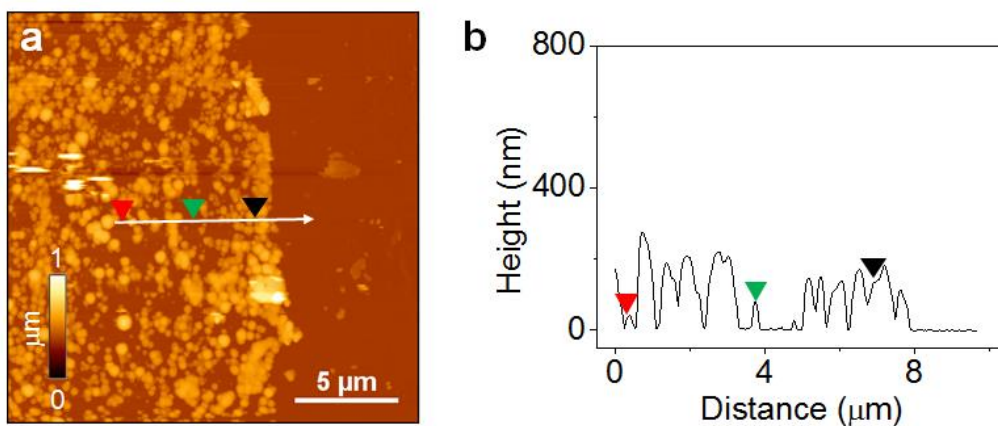


Figure S15. Effect of high concentration on Fe^{III}-TA film formation on planar substrate. (a) AFM height image of a scratched zone of an Fe^{III}-TA film formed on a glass substrate. (b) Corresponding height profile of the Fe^{III}-TA film.

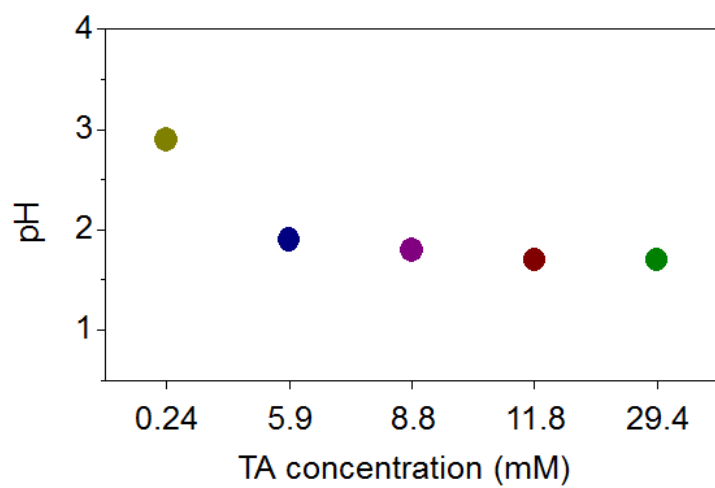


Figure S16. Concentration-dependent pH of the Fe^{III}-TA solution. The TA:Fe^{III} molar ratio is constant (1:1.6).

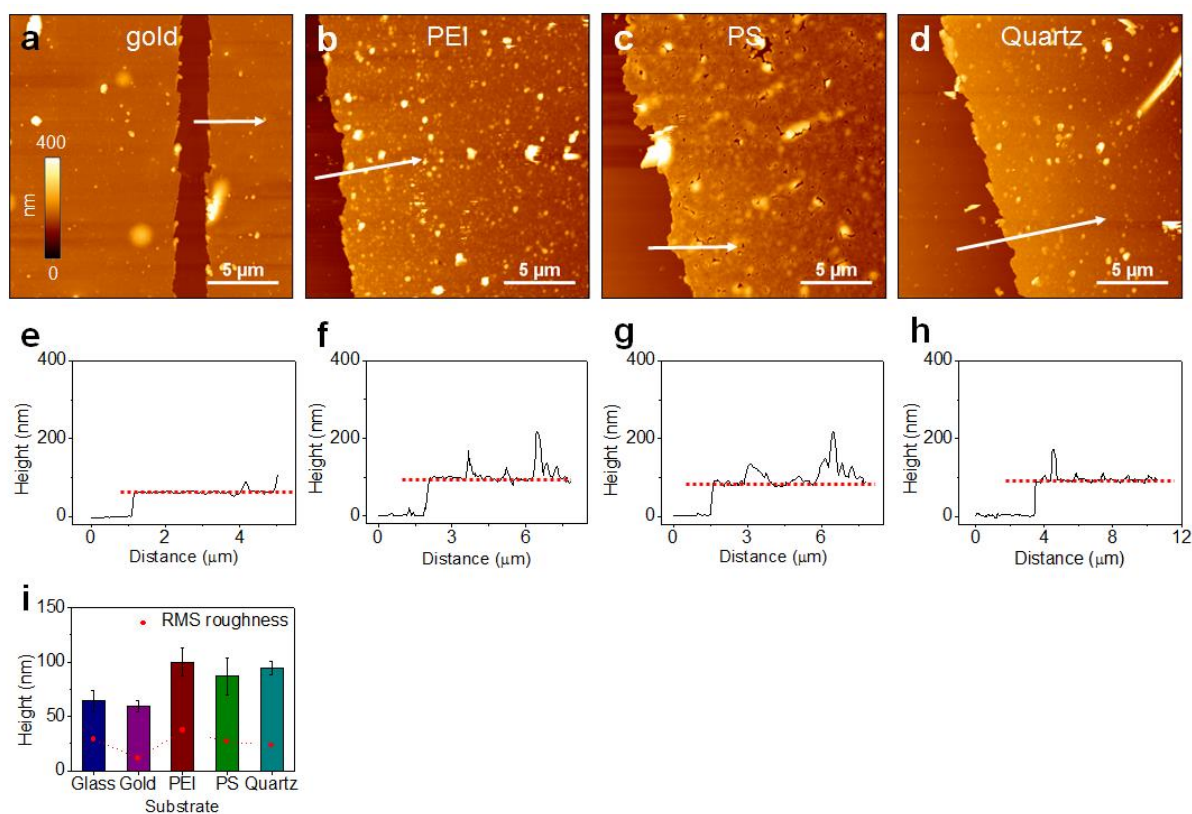


Figure S17. Effect of substrate on Fe^{III}-TA film formation. (a–h) AFM images and corresponding height profiles of a scratched zone of Fe^{III}-TA films grown on different substrates: Gold-coated glass (a, e), PEI-coated glass (b, f), PS-coated glass (c, g), and Quartz (d, h). (i) Effect of substrate on Fe^{III}-TA film formation as measured by AFM height profiles seen in (a–h). Thick films were deposited on both positively charged and hydrophobic surfaces.

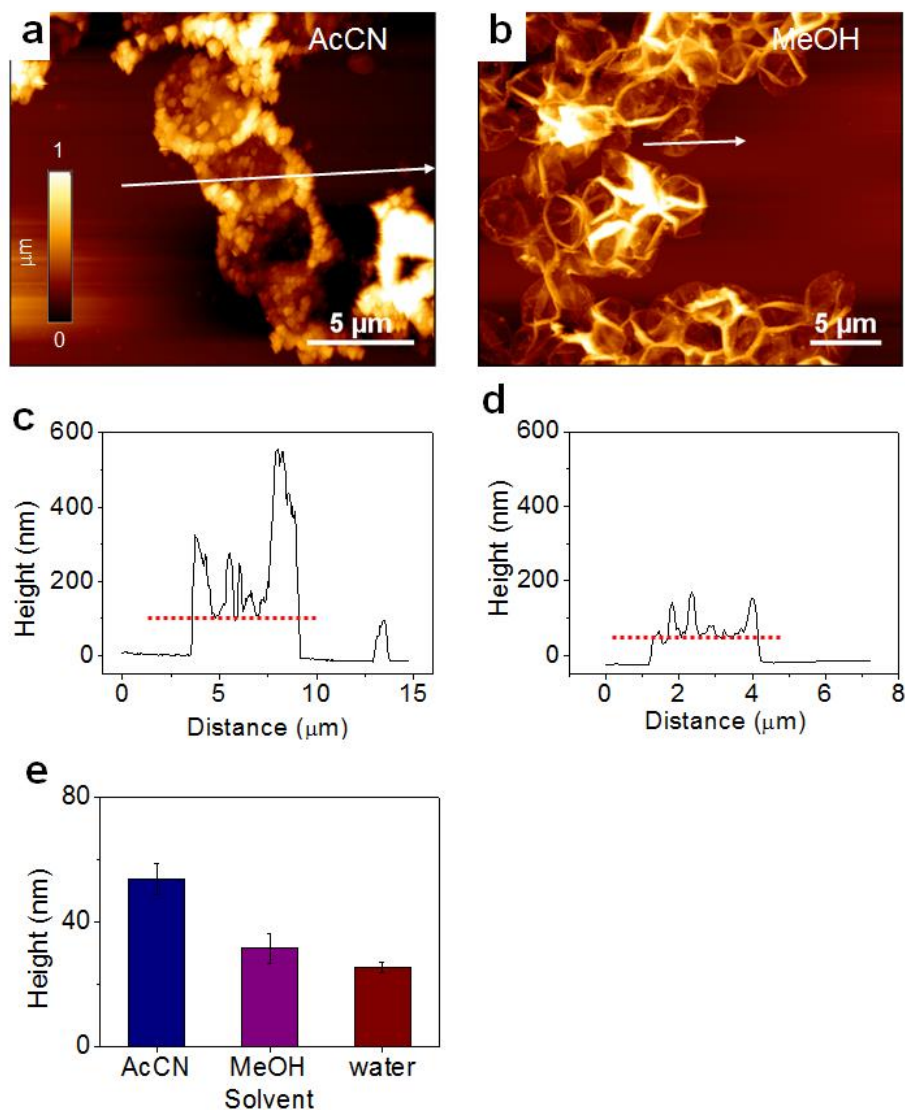


Figure S18. Effect of solvent on Fe^{III}-TA film formation. (a–d) AFM height images and corresponding height profiles of Fe^{III}-TA capsules prepared in AcCN (a, c) and MeOH (b, d). (e) Effect of solvent on Fe^{III}-TA film formation as measured by AFM height profiles seen in (a–d). Film formation in AcCN produced aggregated species in solution, suggesting that the stability of Fe^{III}-TA complexes in solution could influence film growth.

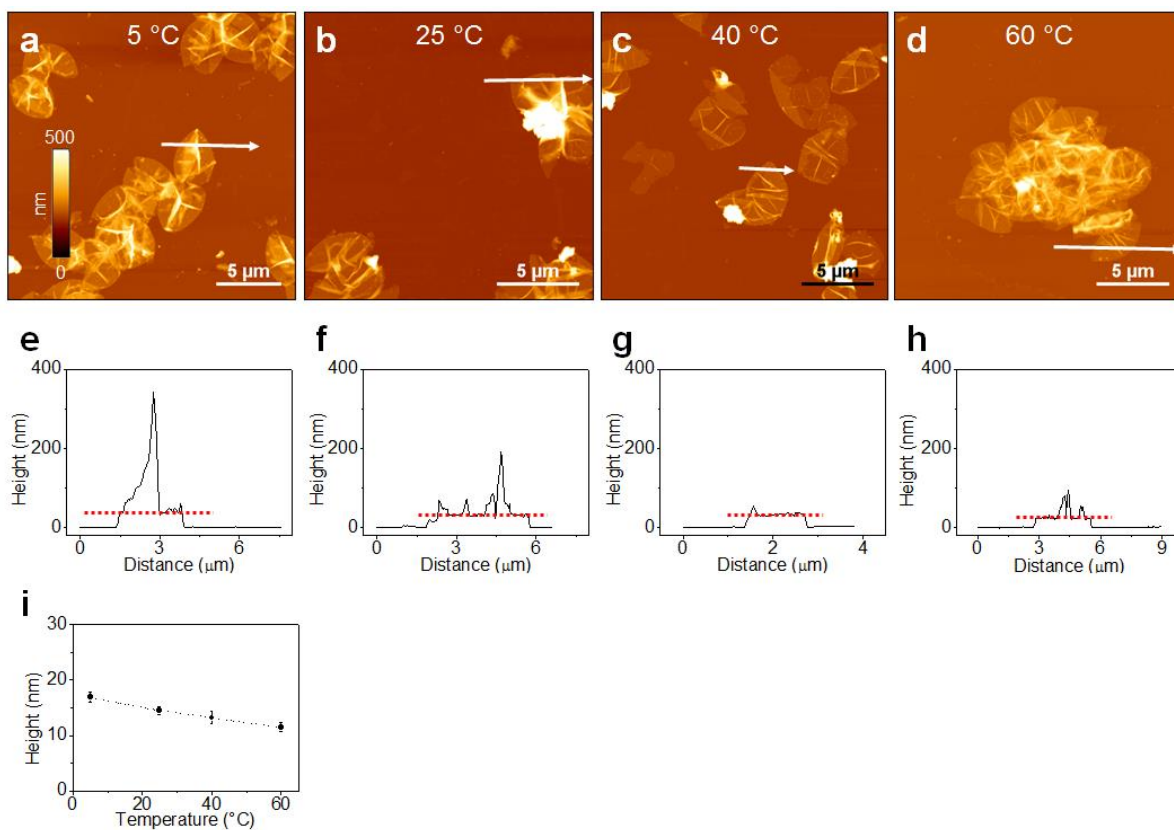


Figure S19. Effect of temperature on Fe^{III} -TA film formation on sacrificial templates. a–h) AFM height images and corresponding height profiles of hollow Fe^{III} -TA capsules prepared at varying temperatures: 5 (a, e), 25 (b, f), 40 (c, g), and 60 °C (d, h). (i) Effect of temperature on Fe^{III} -TA film formation as measured by AFM height profiles seen in (a–h).

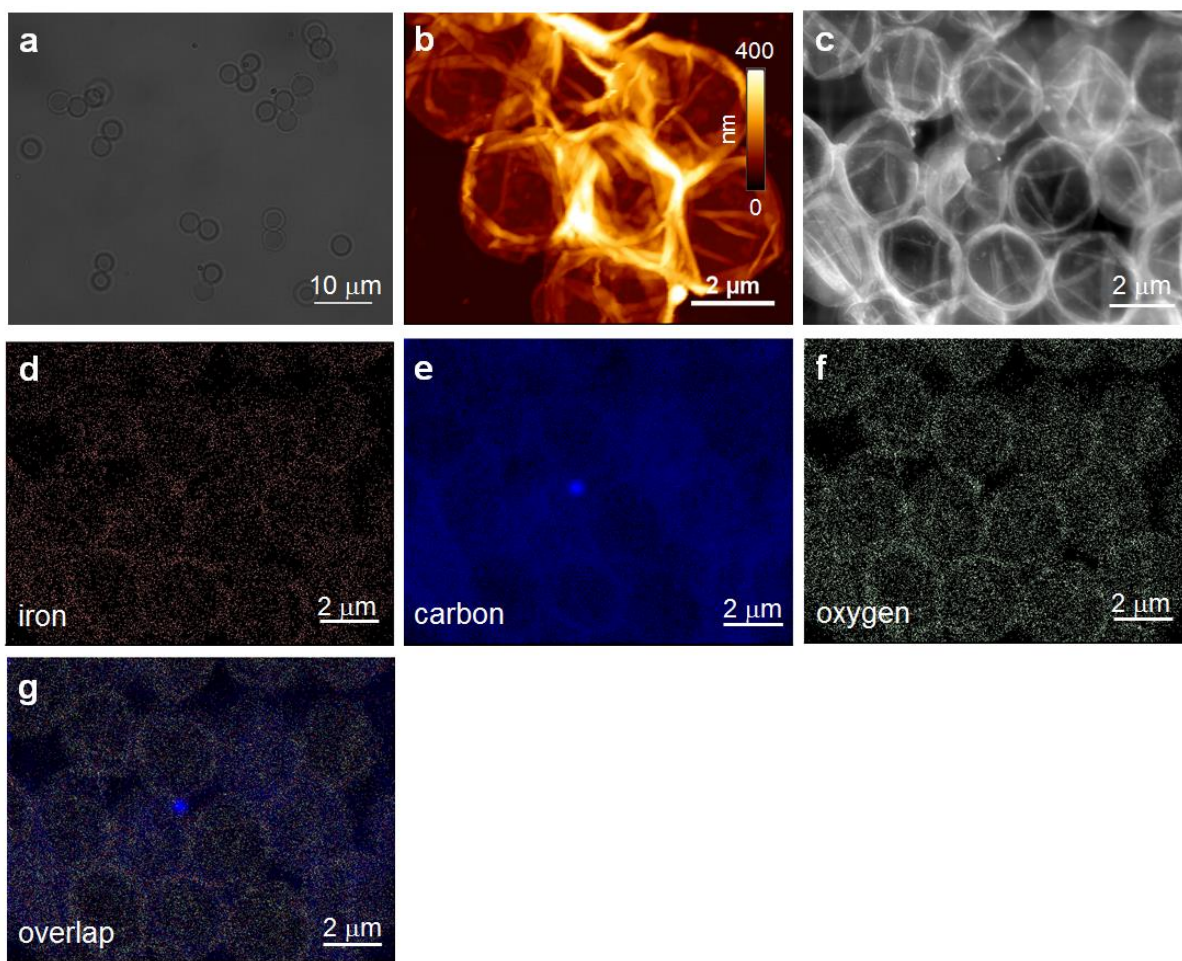


Figure S20. Hollow capsule formation using sacrificial PS particles. (a) DIC image of Fe^{III}-TA capsules. (b) Representative AFM image of the Fe^{III}-TA capsules. (c-g) HAADF TEM, and EDX elemental mapping images of the Fe^{III}-TA capsules.

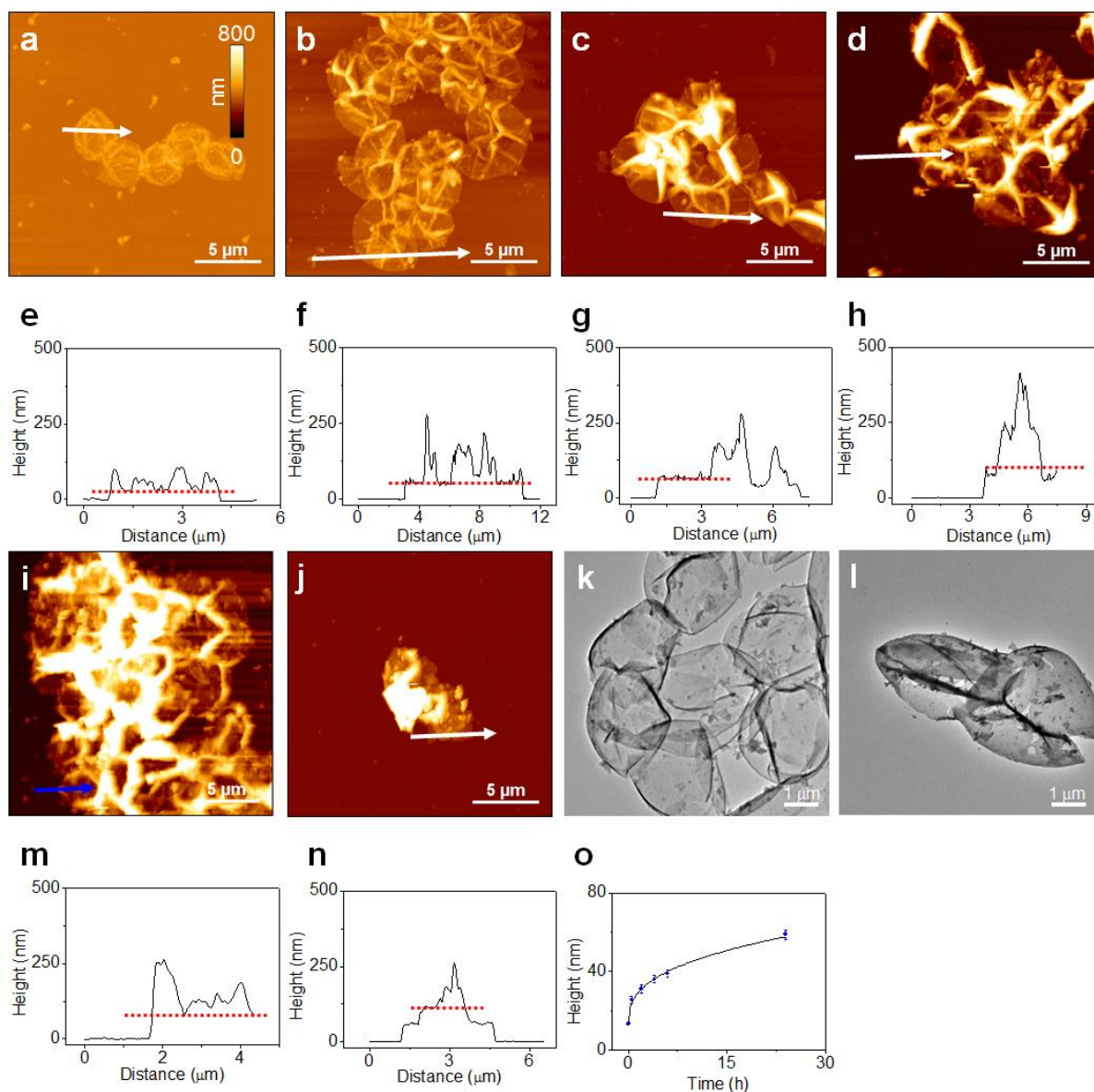


Figure S21. Time-dependent thickness profiles of Fe^{III}-TA capsules. (a–d, i, k) AFM images of Fe^{III}-TA capsules at different immersion times. (e–h, m, n) Corresponding height profiles of the Fe^{III}-TA capsules: 1 min (a, e), 30 min (b, f), 2 h (c, g), 4 h (d, h), 6 h (i, m), and 24 h (j, n). (k, l) TEM images of the capsules at 6 and 24 h, respectively. (o) Thickness profile of Fe^{III}-TA capsules as a function of immersion time as measured by AFM height profiles seen in (a–j, m, n).

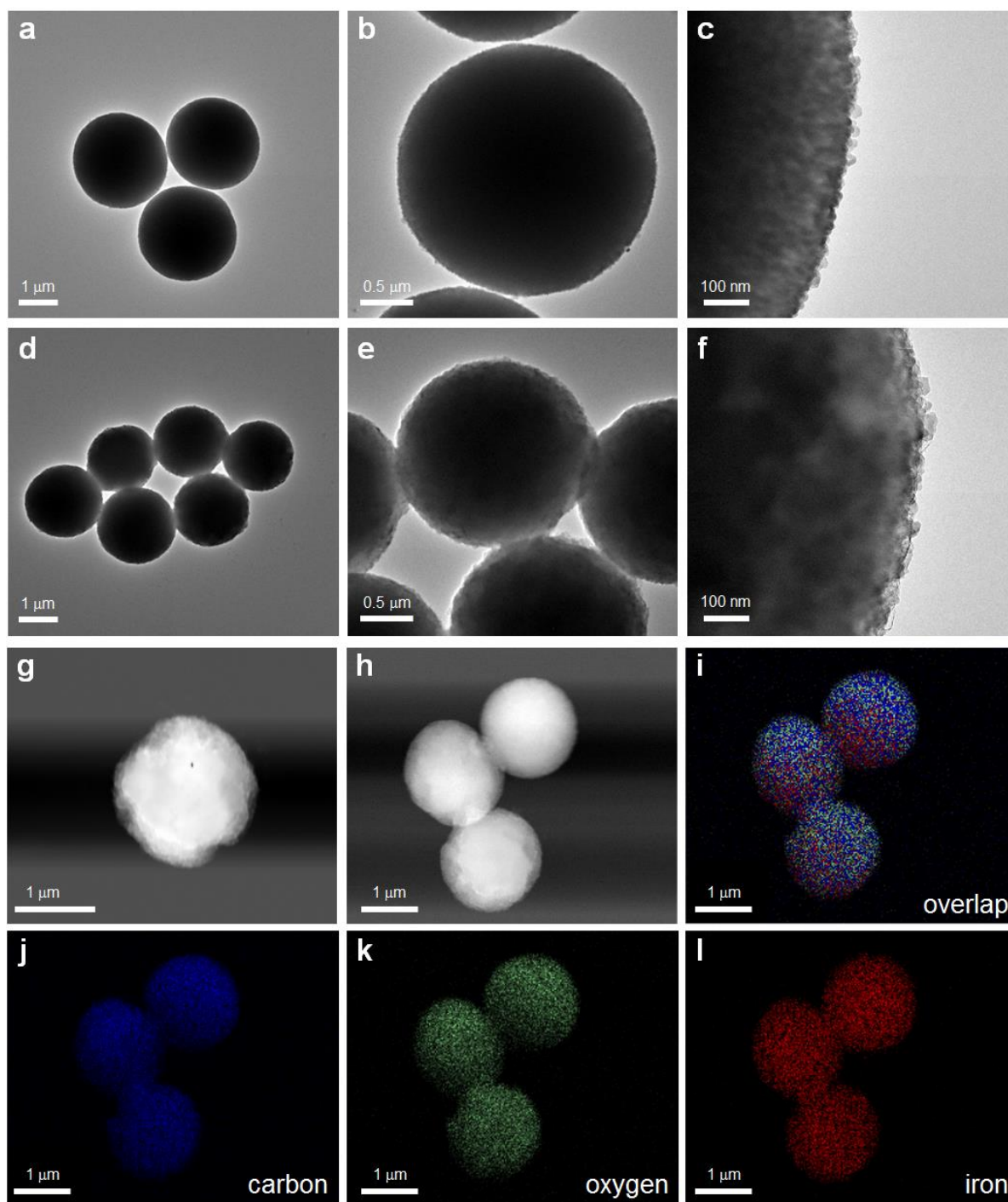


Figure S22. Replica particle formation on sacrificial templates. (a–c) TEM images of CaCO_3 template particles. (d–l) TEM, HAADF, and EDX elemental mapping images of Fe^{III} -TA replica particles.

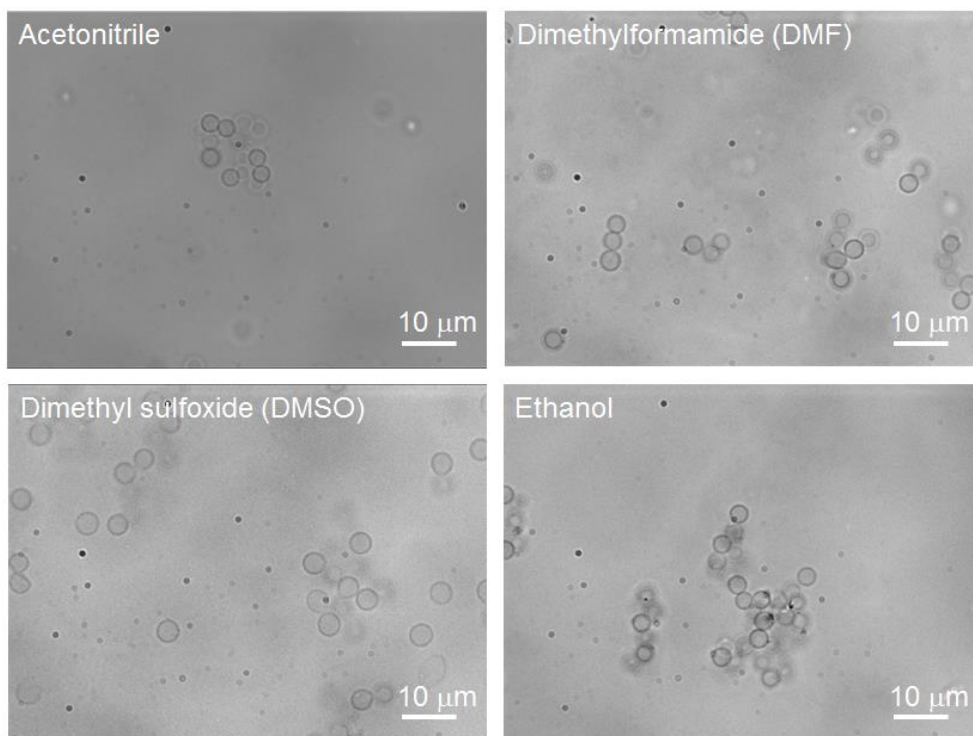


Figure S23. DIC images of Fe^{III}-TA capsules in organic solvents.

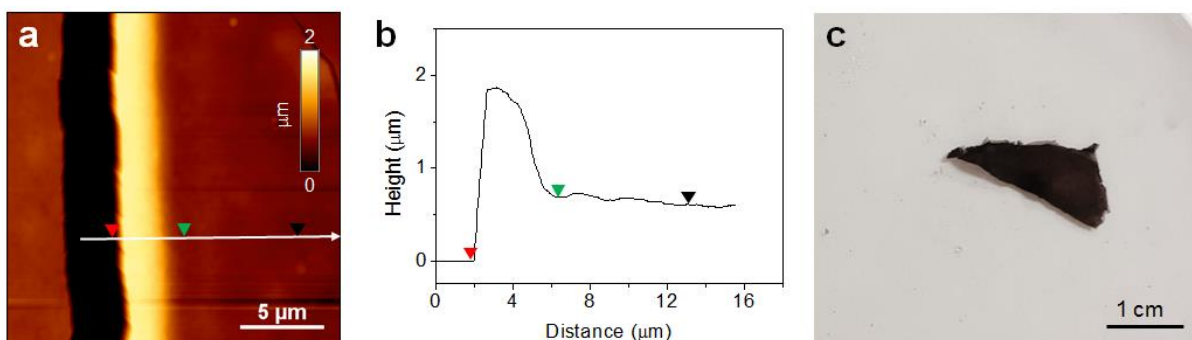


Figure S24. Characterization of free-standing macroscopic Fe^{III}-TA material at different immersion times. (a, b) AFM height images and corresponding height profiles of the Fe^{III}-TA film after 65 h of immersion. (c) Digital photograph of the free-standing macroscopic material in THF after 162 h immersion in the purified Fe^{III}-TA solution.

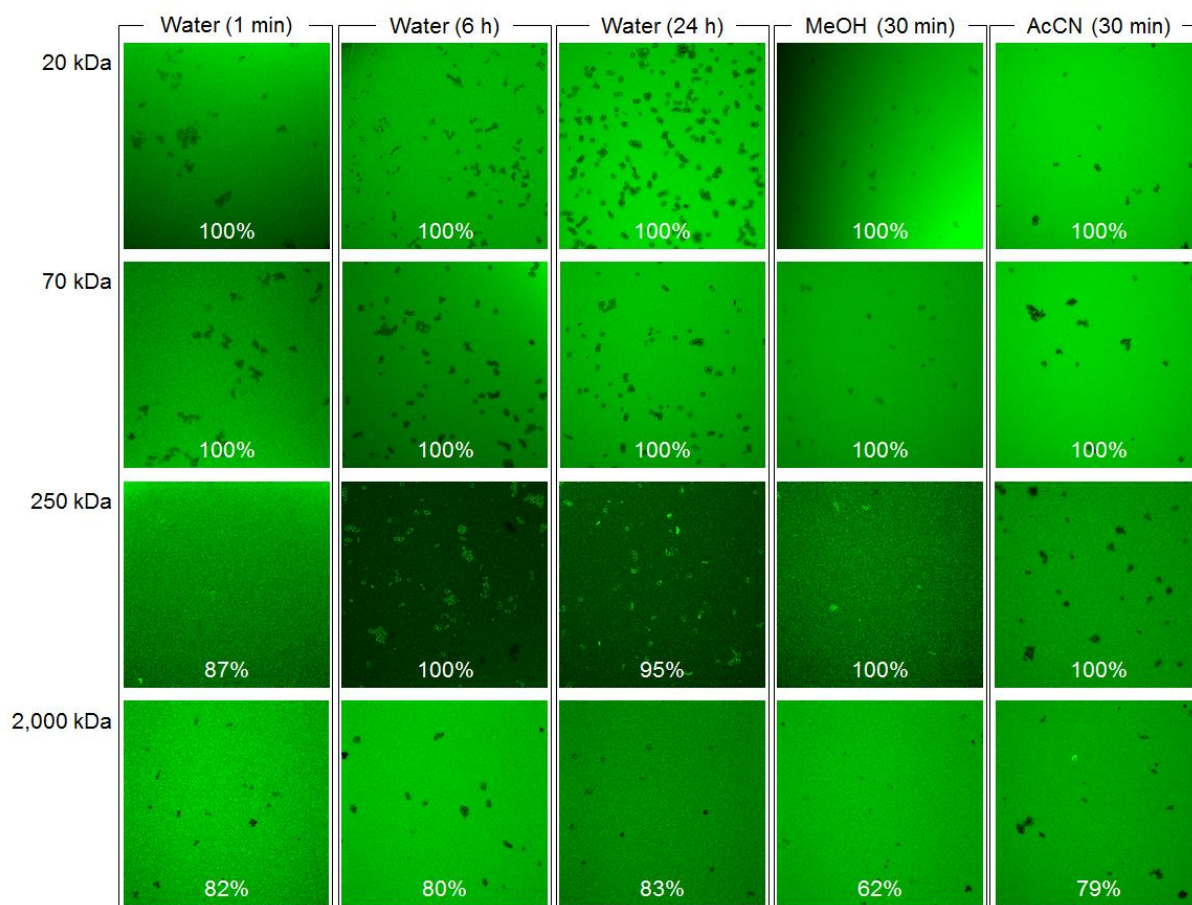


Figure S25. Molecular weight-dependent permeability of Fe^{III}-TA capsules. CLSM images of the Fe^{III}-TA capsules (reaction for 1 min, 6 h, and 24 h in water and 30 min in MeOH and AcCN, respectively) incubated with FITC-dextran (20, 70, 250, and 2,000 kDa). Capsules with dark interiors were considered to be impermeable, whereas capsules with interiors of similar fluorescence intensity to that of the outer environment were considered to be permeable.

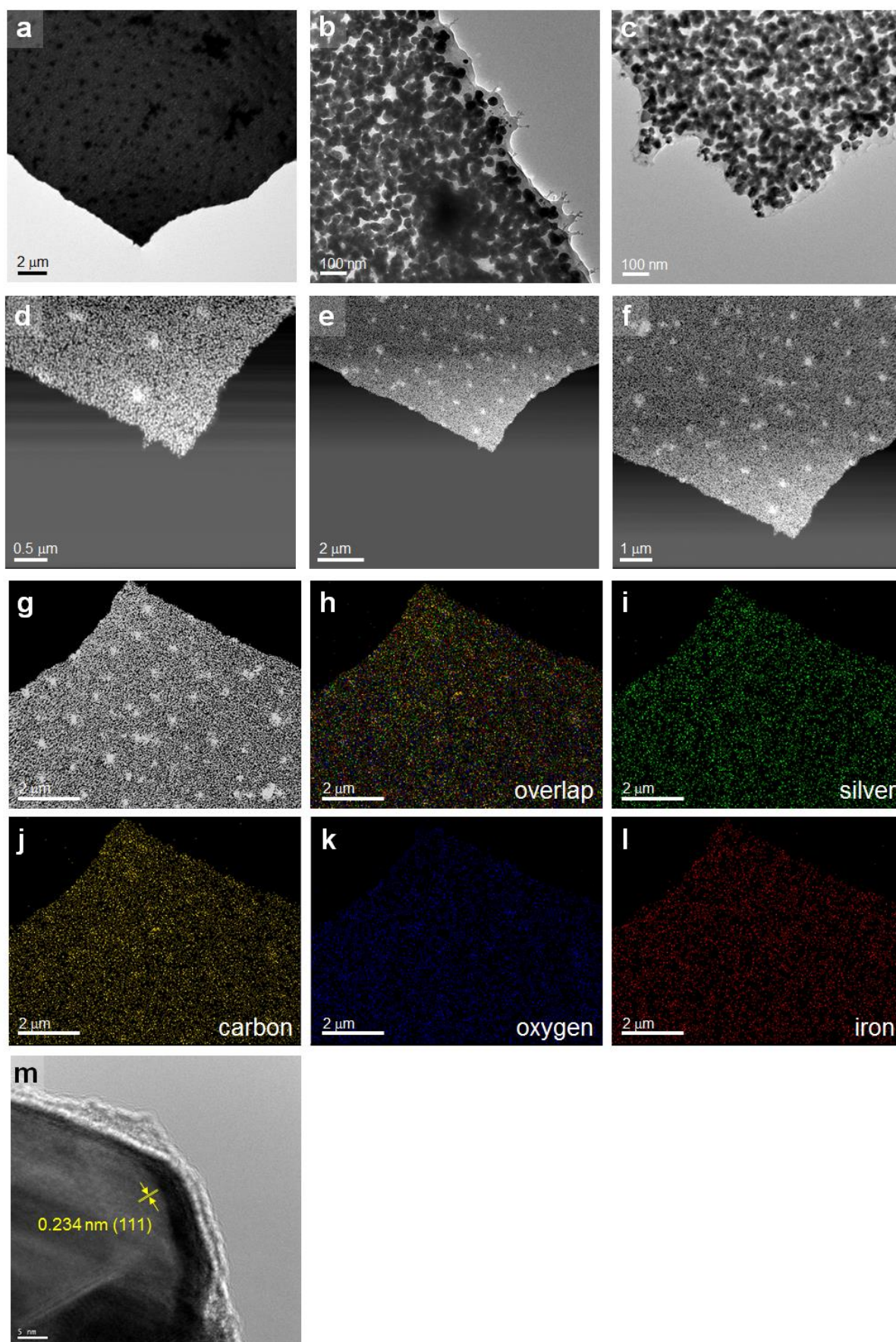


Figure S26. Electron microscopy images of free-standing silver nanoparticle (AgNP) films.

(a-l) Bright-field, HAADF, and EDX elemental mapping images of AgNP-functionalized macroscopic Fe^{III}-TA materials. (m) Silver nanoparticles on the surface of Fe^{III}-TA material. The lattice spacing of 0.234 nm corresponds to the (111) plane of silver.⁵

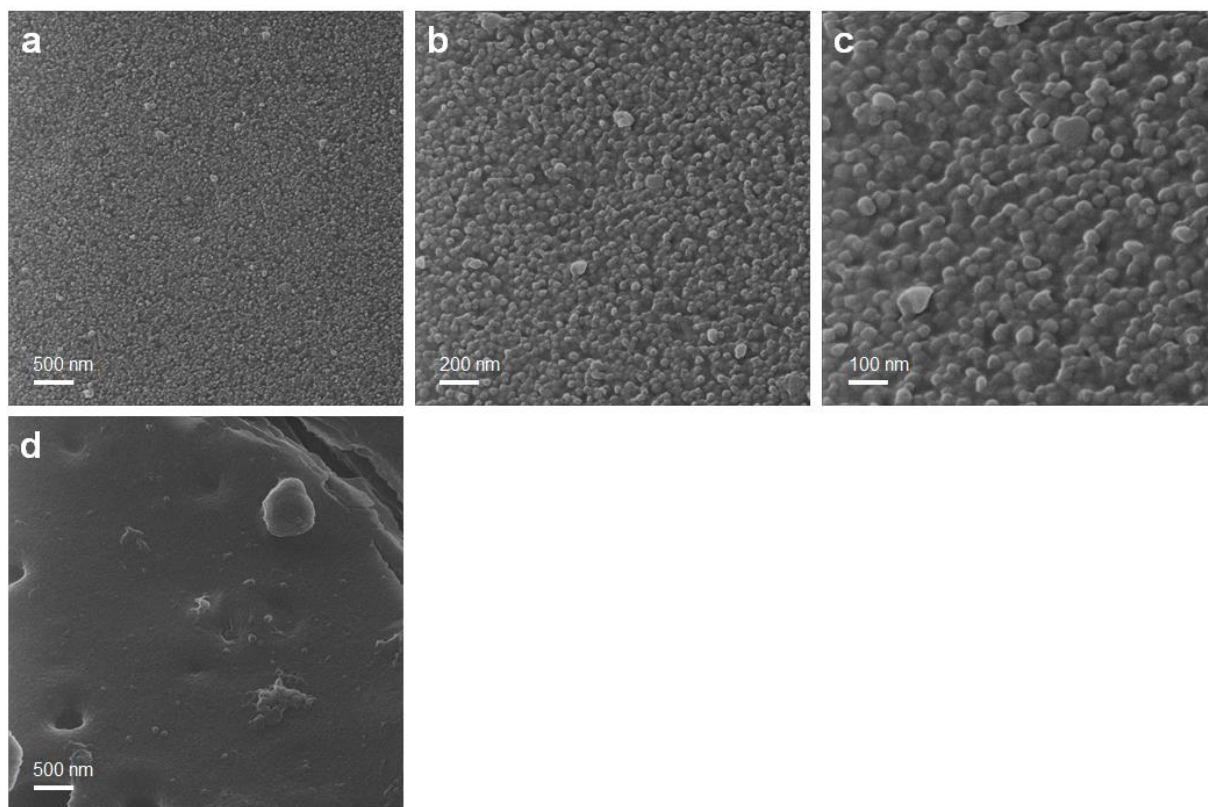


Figure S27. Scanning helium ion microscopy images of free-standing AgNP films: (a–c) AgNP-functionalized macroscopic Fe^{III}–TA materials and (d) free-standing Fe^{III}–TA material before being treated with silver nitrate.

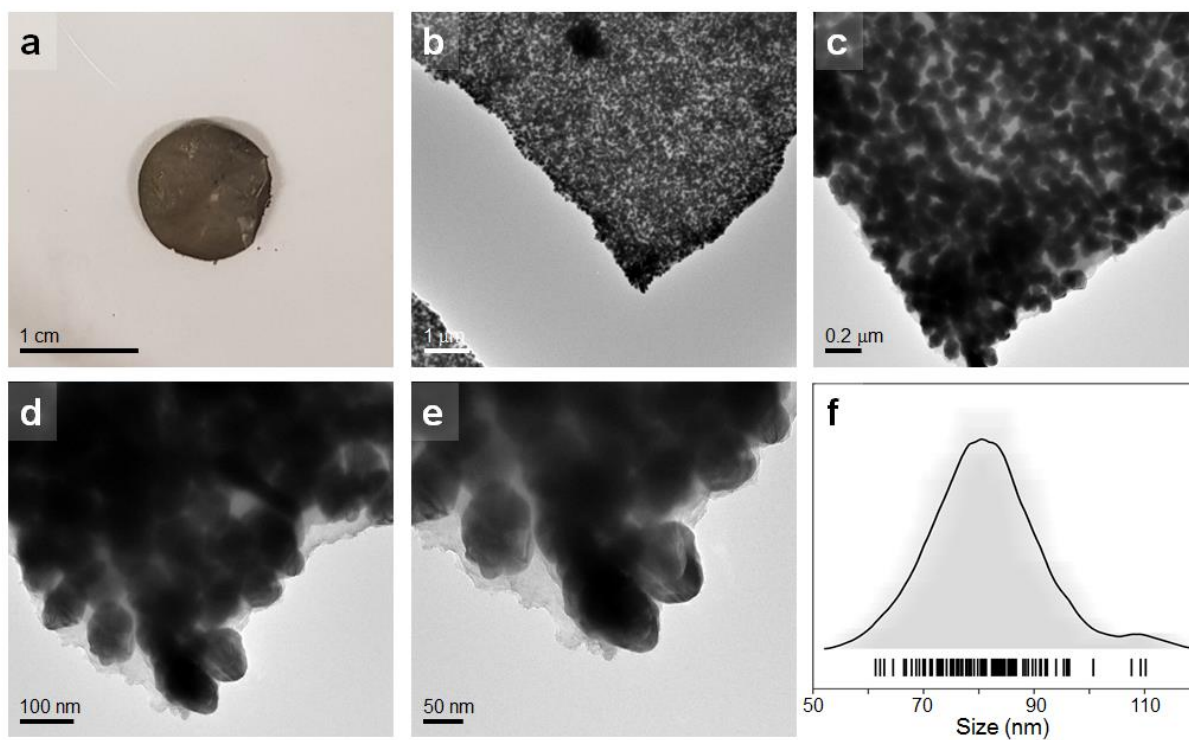


Figure S28. Digital photograph and TEM images of AgNP-functionalized macroscopic Fe^{III}-TA materials after 3 day immersion in Ag(I) salt solution. (a) Digital photograph of the free-standing AgNP film. (b–e) TEM images of the AgNPs on the surface of the Fe^{III}-TA materials. (f) Size histogram of AgNPs; a size distribution of 81 ± 10 nm was determined from analysis of 100 NPs.

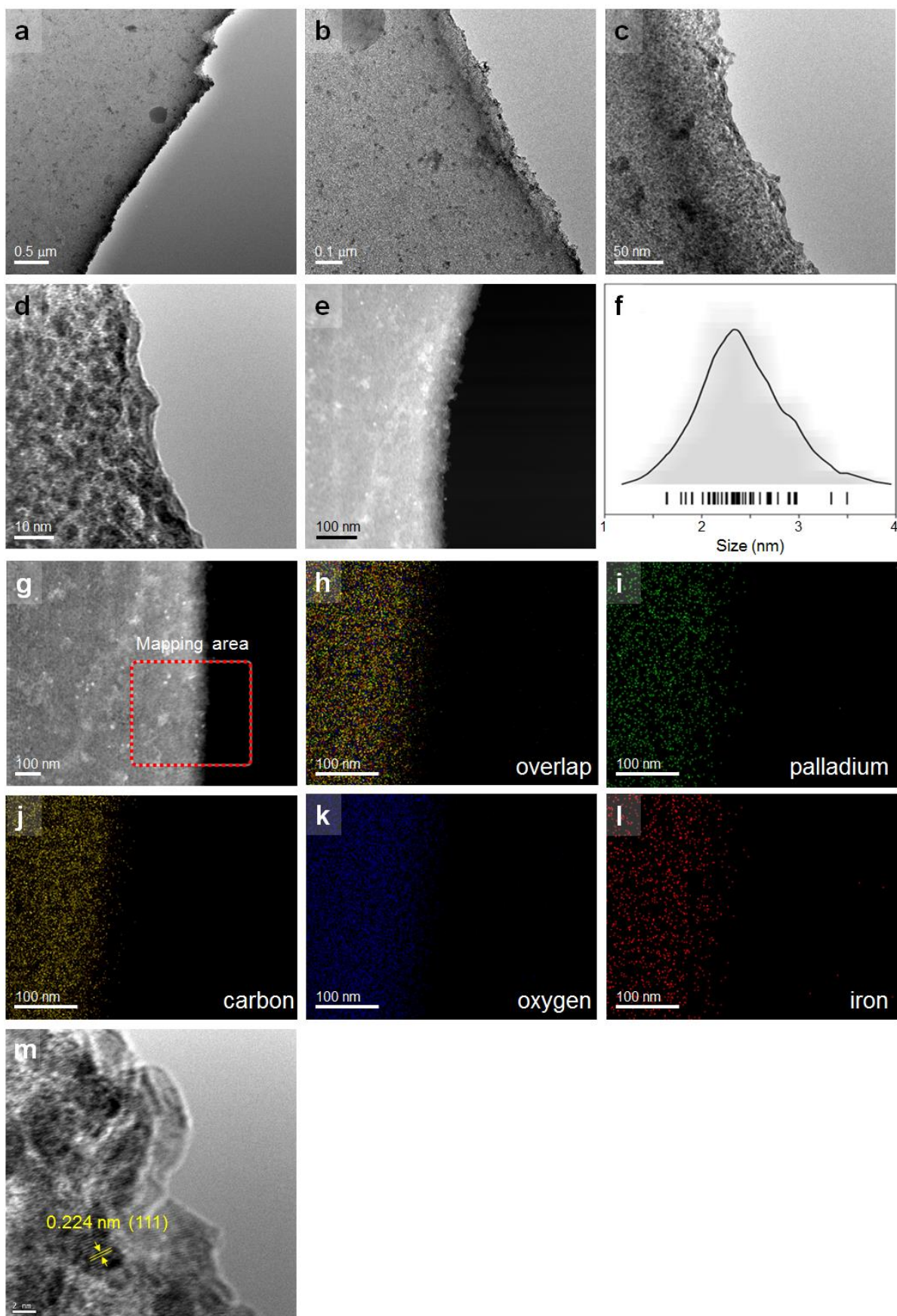


Figure S29. Electron microscopy images of free-standing palladium nanoparticle (PdNP) films and size histogram of PdNPs. (a–d, e, g, h–l) Bright-field, HAADF, and EDX elemental S43

mapping images images of PdNP-functionalized macroscopic Fe^{III}-TA materials. (f) Size histogram of PdNPs; a size distribution of 2.4 ± 0.4 nm was determined from analysis of 50 NPs. (m) Palladium nanoparticles on the surface of Fe^{III}-TA material. The lattice spacing of 0.224 nm corresponds to the (111) plane of a face-centered cubic metallic Pd(0).⁶

Section S11: Supporting references

- (1) Hutter, J. L.; Bechhoefer, J. Calibration of Atomic-Force Microscope Tips. *Rev. Sci. Instrum.* **1993**, *64*, 1868–1873.
- (2) Dimitriadis, E. K.; Horkay, F.; Maresca, J.; Kachar, B.; Chadwick, R. S. Determination of Elastic Moduli of Thin Layers of Soft Material Using the Atomic Force Microscope. *Biophys J.* **2002**, *82*, 2798–2810.
- (3) Ejima, H.; Richardson, J. J.; Liang, K.; Best, J. P.; van Koevorden, M. P.; Such, G. K.; Cui, J.; Caruso, F. One-Step Assembly of Coordination Complexes for Versatile Film and Particle Engineering. *Science* **2013**, *341*, 154–157.
- (4) Moulder, J. F.; Stickle, W. F.; Sobol, P. E.; Bomben, K. D. *Handbook of X-Ray Photoelectron Spectroscopy: A Reference Book of Standard Data for Use in X-Ray Photoelectron Spectroscopy*; Physical Electronics: Eden Prairie, MN, 1995.
- (5) Li, B.; Wen, X.; Li, R.; Wang, Z.; Clem, P. G.; Fan, H. Stress-Induced Phase Transformation and Optical Coupling of Silver Nanoparticle Superlattices into Mechanically Stable Nanowires. *Nat. Commun.* **2014**, *5*, 4179.
- (6) Yun, G.; Pan, S.; Wang, T.; Guo, J.; Richardson, J. J.; Caruso, F. Synthesis of Metal Nanoparticles in Metal–Phenolic Networks: Catalytic and Antimicrobial Applications of Coated Textiles. *Adv. Healthcare Mater.* **2018**, *7*, 1700934.